PEOPLE'S DEMOCRATIC REPUBLIC OF ALGERIA
MINISTRY OF HIGHER EDUCATION AND SCIENTIFIC RESEARCH
MOHAMED BOUDIAF UNIVERSITY - M'SILA

FACULTY OF SCIENCE AND TECHNOLOGY
DEPARTMENT OF ELECTRICAL ENGINEERING
N°: ER-04

FIELD: SCIENCE AND TECHNOLOGY
SECTOR: ELECTROTECHNIC
OPTION: RENEWABLE ENERGIES IN ELECTRICAL ENGINEERING

Thesis presented for obtaining

Academic Master's degree

By:

Z I A N I Z I A N E & BELKAIBECH YOUNES

Titled:

Futoshiki technique for PV array power optimization Under partial shading conditions

Presented before the jury composed of:

Dr.Messaoud MAYOUF	University of Mohamed Boudiaf - M'sila	President
Pr.Djamel SAIGAA	University of Mohamed Boudiaf - M'sila	Supervisor
Dr.Abdelouadoud LOUKRIZ	University of Mohamed Boudiaf - M'sila	Co Supervisor
Dr.Abdelhakim IDIR	University of Mohamed Boudiaf - M'sila	Examiner

Academic year: 2022/ 2023

Thank

I.1 Thanks:

We thank Allah for giving us good health and the courage to carry out this work successfully. Enabling us to successfully complete this endeavor.

We would like to extend our appreciation to Professor Pr. Djamel Saigaa for proposing an intriguing master's topic and providing guidance.

We are sincerely thankful to Mr. Dr. Abdelouadoud Loukriz for sharing information, offering advice, and assisting us throughout this task. We also acknowledge the significant contributions of all the teachers who have played a part in our academic journey. Lastly, we extend our heartfelt thanks to our families, friends, and colleagues for their support and encouragement.

I.2 Dedications

In our master's thesis dedication, we express our deepest gratitude and dedication to our family and friends for their continued support throughout our academic journey. We acknowledge their unwavering belief in our abilities their presence in difficult times and their encouragement to follow our dreams. We dedicate our master's degree to them as a sign of their love and support. Their unwavering dedication has been the driving force behind our accomplishments and we are so grateful to have them in our lives.

[ZIANE & YOUNES]

I.3 Summary

Summary

Summary

Summary

List of symbols and abbreviations

Voc	Open-circuit voltage (V)
Isc	Short-circuit current (A)
V_d	Diode voltage (V)
I	the current through the diode (A)
I_0	the reverse saturation current (A)
V	the applied voltage across the diode (V)
K	Boltzmann's constant (1.381*10-23 J/K),
T	the temperature in Kelvin (K)
Q	the electron charge (1.602*10-19 C)
Vmp	Maximum power voltage(V)
Imp	Maximum power current(A)
MPPT	Maximum Power Point
PMPP	Point of Maximum Power Point
STC	standard test circumstances
FF	Fill factor
H	Conversion efficiency
R_s	series resistance of the solar cell (Ω)
N	ideality factor (1<n< 2)
R_{sh}	shunt resistance of the solar cell (Ω)
I_{cref}	the reference current (A)
G	Solar irradiation W/m^2
G_{STS}	Solar irradiation in standard test circumstances W/m^2
N_s	Number of cells in series.
N_p	Number of cells in parallel.
P	the power (w)
U	Tensions (V)
PS	Partial shading
PV	photovoltaic panels
SP	Serial-Parallel

TCT	Total-Cross-Tied
BL	Bridge Linked
HC	Honey Comb
GMPP	Global Maximum Power Point
ML	mismatch loss
SF	shading factor
C	Columns
R	Rows
I_m	the current produced by the module
Vmx	the voltage of the x^{th} row
SW	Short and wide
LW	Long and wide
SN	Short and narrow
LN	Long and narrow

List of figures

CHAPITRE I: General information on solar photovoltaic system

Summary

CHAPITREII: Study and comparison of the different configurations under the effect of partial shade

Summary

CHAPITRE III: Power optimization of a PV array in a partially shaded TCT configuration by using the Futoshiki technique

List of Table

GENERAL INTRODUCTION

GENERAL INTRODUCTION :

In recent years, there has been a significant global increase in energy demand across various aspects of life, particularly electricity. unfortunately, a large portion of this electricity is still derived from fossil fuels, which have a detrimental environmental impact., faced with the global challenge posed by fossil fuels and their effects on climate change.[1]

In addition to there is another problem such as the problem of isolated locations, where many people are scattered in isolated areas. In these areas the electricity supply is only dependent on independent diesel generation systems. Apart from the increasing cost of fuel, the extension of the electricity grid is very expensive, and the additional cost of fuel supply increases greatly with isolation, which makes power generation economically very expensive, which reflects the implementation of a solution Perfect as decentralized power generation.[2]

to solve this problem, Measures have been intensified in the electricity production sector in order to develop clean and inexhaustible renewable energy sources, which represent a considerable source of energy worldwide Many countries have recognized this and made substantial investments, showing promising progress in achieving a balance between energy production and consumption while preserving the environmental equilibrium of the planet. among the various renewable energy options, solar power stands out as the most promising source. [3]

however, it is known that the electricity generated by photovoltaic modules can be significantly reduced under certain circumstances, such as shading and suboptimal operation. In this dissertation, our focus was on investigating the effects of shading on energy production and exploring methods to minimize its impact on photovoltaic energy generation.

The contributions of this research work are as follows:

- Development of shade dispersion method: The research proposes a technique for dispersing shading effects in TCT configurations of PV systems. By using the Futoshiki technique, it is possible to optimize the arrangement of PV panels to minimize power losses due to shading and improve the overall efficiency of the system.
- Comparative analysis of TCT and Futoshiki configurations: The work conducts a comparative analysis between traditional TCT configurations and configurations optimized by the Futoshiki technique. This highlights improvements in terms of energy yield, maximum power point, and mismatch losses.
- Study of performance under different shading scenarios: The research considers multiple conventional shading scenarios and evaluates the performance of TCT and

Futoshiki configurations in each scenario. This helps determine the effectiveness of the Futoshiki technique in dispersing shading effects and identify situations where it brings the most significant advantages.

- Validation through simulation: Simulations are performed using MATLAB Simulink to assess the performance of TCT and Futoshiki configurations. The obtained results allow for quantitative comparison of the two approaches and analysis of the impact of the Futoshiki technique on the overall performance of the PV system.
- Exploration of larger-scale configurations: The work extends the analysis to larger PV configurations using a 9x9 PV panel array. This allows for evaluating the effectiveness of the Futoshiki technique in more complex scenarios and determining its adaptability to large-scale installations.

By combining the TCT approach with the Futoshiki technique, this work provides significant contributions to the optimization of PV panel configurations. It offers insights to enhance the energy efficiency of PV systems, reduce power losses due to shading, and facilitate more effective utilization of solar energy. These contributions can guide the development of new approaches to PV system design and support the transition towards clean and renewable energy.

The dissertation is divided into three chapters:

Chapter One:

The first chapter, will provide an overview of electric power generation using photovoltaics. It will cover their electrical properties and photovoltaic modeling and the effect of lighting and temperature on their performance, and the configuration of photovoltaics in series and parallel. and mentioning the advantages and disadvantages. for the photovoltaic system.

Chapter two:

This chapter studies the effect of partial shading on the photovoltaic unit, and we dealt with and discussed four configuration scenarios for photovoltaic cells, then presented a comparison between the different configurations and deduced the best configuration.

Chapter three:

In this chapter, we introduced a definition of (futoshiki technique), which we applied to TCT configurations in different shading scenarios in order to reduce the effect of shading and improve production efficiency.

Finally, we end this note with a general conclusion on the subject.

I) CHAPITRE I: General information on solar photovoltaic system

I.1 INTRODUCTION:

The sustained human need for energy has always pushed him to extract energy and to research its sources and methods of obtaining it, especially solar energy. Responsible for the discovery of the photovoltaic effect in 1839 is the physicist EDMOND BECQUEREL, who discovered the possibility of converting light energy into electricity. This phenomenon is based on semiconductor technology. It consists in using the energy of the photons to release electrons that create a potential difference between the terminals of the cell, which becomes a source of constant electric current. The first applications date back to the 1960s with equipment for space satellites [4]

In this chapter, we will use some basic concepts in the field of photovoltaic cells, and therefore we will touch on concepts related to the photovoltaic energy source and photovoltaic installations, and we will study the functional principle of the photovoltaic generator under the photovoltaic cell. Under normal conditions (G = 1000W / m2, T = 25 ° C), we deal with the effect of temperature and irradiation intensity on PV power, for validation, MATLAB tool is used to simulate the behavior of a photovoltaic cell under different metrological conditions

I.2 Solar energy:

Solar energy is the energy that is generated from solar irradiation. It is a form of renewable energy that can be harnessed through various technologies, such as photovoltaic solar panels or solar thermal systems.

as it is predicted that the sun will keep emitting energy for billions of years. Additionally, it is a safe and eco-friendly substitute for fossil fuels, which release harmful pollutants and advance climate change. The sun sends irradiation to the surface of the earth, which represents approximately 8400 times the energy consumption of humanity each year. According to reliable observations, 1366 W/m2 is the solar constant, or the average solar energy density directly outside of the Earth's atmosphere. This corresponds to an instantaneous power received of 1 kilowatt peak per square meter (kWp/m2) distributed over the entire spectrum, from ultraviolet to infrared. [5]

Solar energy is produced and used in several ways:

I.2.1 Solar thermal energy:

Solar thermal energy is a form of renewable energy that uses the heat from the sun to produce electricity or heat. Solar thermal energy is often used to heat domestic water or

buildings, but it can also be used to produce electricity on a large scale in solar thermal power plant.

I.2.2 photovoltaic solar energy:

Photovoltaic solar energy is a renewable energy technology that uses solar panels to convert solar irradiation directly into electricity. This electricity can be used to power homes, businesses, and other applications. Photovoltaic solar energy is a clean and sustainable source of energy that produces no emissions, reduces dependence on fossil fuels, and contributes to a more sustainable energy system.[5]

I.2.3 Solar irradiation:

Refers to the amount of solar irradiation that is received by a specific surface area, usually measured in watts per square meter (W/m^2). Solar irradiation is affected by factors such as latitude, altitude, and weather conditions, and it varies throughout the day and over the course of the year. Understanding the level of solar irradiation at a particular location is important for determining the potential for solar energy production and for designing solar energy systems such as photovoltaic solar panels or solar thermal systems.

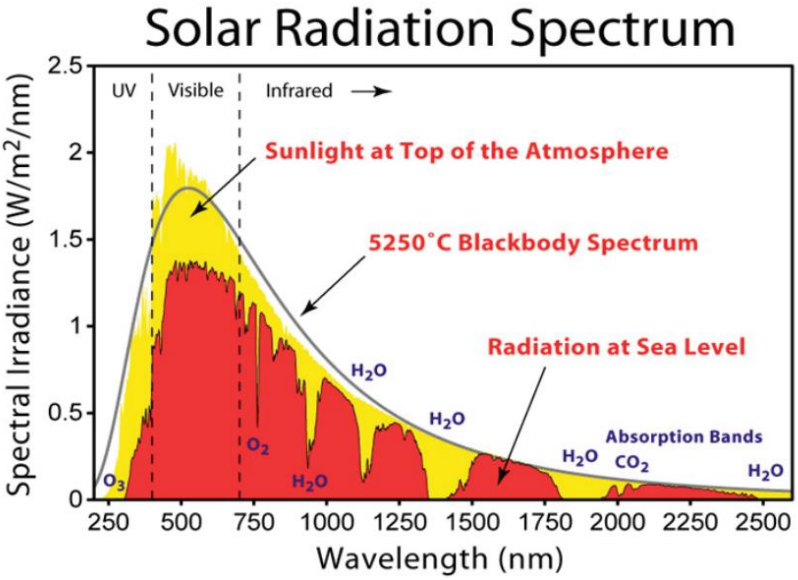

Figure I 1 Solar irradiance spectrum above atmosphere and at surface[6]

There are four main types of solar irradiation:

I.2.3.1 Direct irradiation:

This is the solar irradiation that reaches a surface directly from the sun, without being scattered or reflected by the atmosphere.

I.2.3.2 Diffuse irradiation:

This is the solar irradiation that has been scattered or reflected by the atmosphere before reaching a surface. It comes from all directions, not just from the sun, and is usually less intense than direct irradiation.

I.2.3.3 Reflected irradiation:

This is the solar irradiation that is reflected off of other surfaces, such as the ground or buildings, before reaching a surface. It can contribute to the total amount of solar energy that reaches a surface, but is usually less intense than direct or diffuse irradiation.

I.2.3.4 Global irradiation:

also known as total irradiation, refers to the total amount of solar irradiation that is received by a horizontal surface at a specific location over a given period of time. It includes both direct and diffuse irradiation as well as any reflected irradiation. [7]

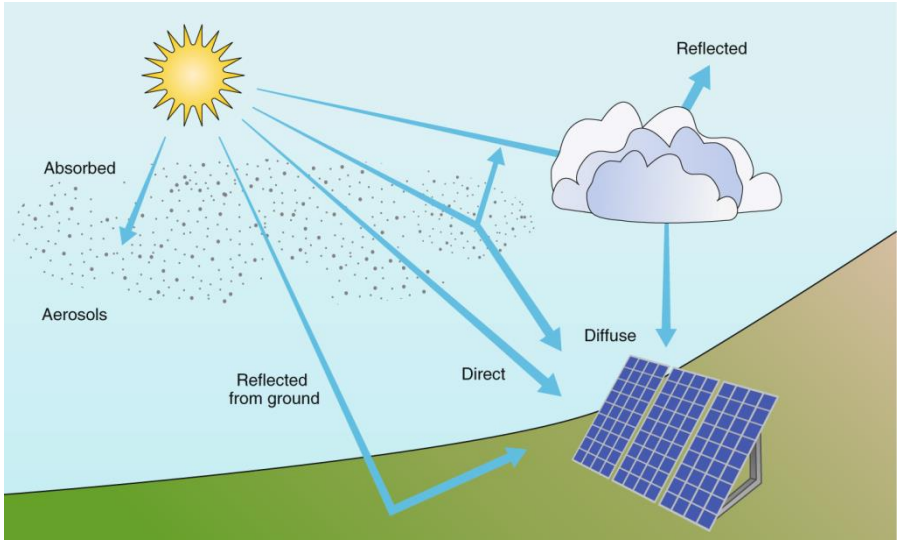

Figure I 2 The different types of solar irradiation[8]

The solar flux received on a surface depends on several factors, including:

- ✓ Latitude:

The amount of solar irradiation received on a surface depends on the latitude of the location. The closer a location is to the equator, the more solar irradiation it receives.

- ✓ Time of day:

  The solar flux received on a surface varies depending on the time of day. The maximum solar irradiation is received at solar noon when the sun is directly overhead.

- ✓ Season:

  The solar flux received on a surface also varies depending on the season. During the summer months, the solar irradiation is higher compared to the winter months.

- ✓ Altitude:

  The solar irradiation is higher at higher altitudes due to the thinner atmosphere which absorbs less solar irradiation.

- ✓ Weather conditions:

  Clouds, haze, and pollution can reduce the amount of solar irradiation that reaches the surface.

- ✓ Orientation:

  The orientation of the surface relative to the sun also affects the amount of solar irradiation received. Surfaces that are oriented towards the sun receive more solar irradiation than those that are not. [9]

I.2.4 Types of solar energy:

Here is a list of the four types of solar energy, with a brief description of each type and its source:

I.2.4.1 Solar photovoltaic energy:

Photovoltaic solar panels are used to turn the sun's light energy into electricity, creating solar photovoltaic energy. [10]

I.2.4.2 Solar thermal energy:

Solar thermal energy is created by storing the heat from the sun and may be used to heat buildings, water, or produce electricity using solar thermal panels.[10]

I.2.4.3 Passive solar energy:

passive solar energy is created by heating and lighting buildings without the need for electricity by utilizing the sun's heat and natural light. [11]

I.2.4.4 Thermodynamic solar energy:

Thermodynamic solar energy is created when the heat from the sun is transformed into mechanical energy by employing mirrors or lenses to concentrate the light on a collecting point. This energy is then utilized to generate electricity. [10]

I.3 Photovoltaic Conversion:

I.3.1 The photovoltaic effect:

Is the physical process that takes place in a semiconductor material when it absorbs photons of light and produces an electrical current. When a photon of light strikes a semiconductor material, such as silicon, it can excite an electron in the material to a higher energy state, allowing it to move freely within the material. A potential difference across the material is produced by the motion of the electron and may be used to produce an electrical current. This is the basis of the operation of a photovoltaic cell, also known as a solar cell, which is used to convert solar irradiation into electrical energy. [12]

I.3.2 The principle of the conversion:

Two distinct doped semiconductor layers are brought into contact in a conventional photovoltaic cell, forming an interface. The lower layer has less electron doping than the upper layer, which has more electrons. When light from the sun strikes the cell, photons are taken up by the top layer and produce electron-hole pairs. The electrons that are liberated by the electron-hole pairs are drawn to the cell's top layer, where they may be gathered and used to power an external circuit. [13]

I.3.3 Photovoltaic cells:

I.3.3.1 Historical overview:

Photovoltaic cells were discovered in 1839 by French scientist Alexander Edmond Becquerel. At the beginning of the 20th century, scientists began working on converting solar energy into electricity using photovoltaic cells. In 1954, American scientists Daryl Chapin, Calvin Fuller and Gerald Pearson developed the first silicon-based solid-state solar cell, which had a conversion rate of 6%. Photovoltaic cells were first used in NASA space programs in the 1960s and 1970s, and later in commercial applications such as solar calculators and garden lights in the 1980s. photovoltaics have continued to evolve and

improve, allowing wider use of solar energy. Today, photovoltaic cells are widely used to generate electricity from solar energy. [14]

I.3.3.2 Definition of the photovoltaic cell:

is an electronic device that converts solar irradiation directly into electrical energy through the photovoltaic effect. It is made of a semiconductor material, usually silicon, that absorbs photons from solar irradiation and emits electrons. The movement of these electrons causes an electric current to flow. Solar cells can be used to generate electricity for a variety of applications, from small electronic devices such as calculators and watches to large power plants that supply electricity to communities. [15]

I.3.4 The different technologies:

There are several different types of photovoltaic cells or solar cells, including:

I.3.4.1 Monocrystalline silicon cells:

Monocrystalline silicon cells have a high degree of efficiency in converting solar irradiation into energy because they are constructed from high-purity silicon with a continuous and uniform crystal structure. PV cells are constructed from thin silicon wafers that have been cut from a single silicon crystal to produce Monocrystalline silicon cells. These cells often have rounded edges, a dark tint, and a homogeneous appearance. They are frequently found in solar panels for both domestic and industrial use. Compared to other types of PV cells, Monocrystalline silicon cells are more efficient, last longer, and have a yield of 12 to 18%, but they cost more to make. [16]

Figure I 3 monocrystalline silicon cell /module [17]

I.3.4.2 Polycrystalline silicon cells:

silicon polycrystalline cells They are created from several silicon pieces that are heated, molded into a block, and then divided into wafers to produce the PV cells. Polycrystalline silicon cells have a distinctive appearance, with a textured blue color and a rough, irregular surface due to the multiple crystals in the material. Their yield ranges from 11 to 15%. Although less efficient than Monocrystalline silicon cells, polycrystalline silicon cells are less expensive to produce. [18]

Figure I 4 Polycrystalline silicon cell/module[17]

I.3.4.3 Thin-film solar cells:

This type of photovoltaic (PV) cell uses solar irradiation to produce electricity. They are made by adding a thin layer of semiconductor material onto a substrate like glass, plastic, or metal. Cadmium telluride, copper indium gallium selenide, and amorphous silicon are semiconductor materials used in thin-film solar cells. Although thin-film solar cells are less efficient than crystalline silicon cells, they are also thinner, lighter, and more flexible, and they have a yield of 6–8%.[19]

Figure I 5 Thin-film solar cells[20]

I.3.5 Modeling a PV cell:

We can simulate the properties of a PV cell by using equivalent electrical circuits. The technique used here is implemented for simulation in MATLAB.

I.3.5.1 The simplest model of a photovoltaic cell:

A diode is connected in parallel to an ideal current source in a photovoltaic cell's equivalent circuit. A current equal to the flux of solar irradiation to which is exposed is delivered by the current source

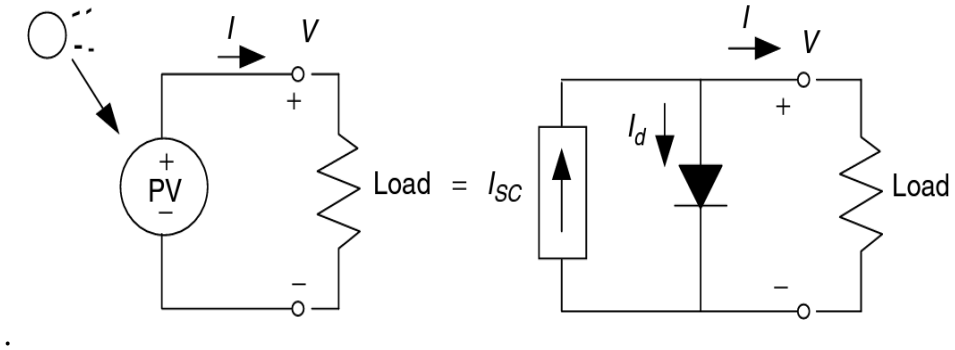

Figure I 6 Basic electrical representation of a solar cell[21]

The photovoltaic system has two important parameters:

Short-circuit current: Open-circuit voltage:

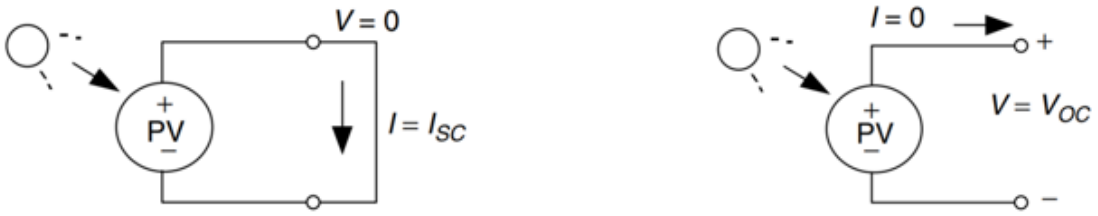

Figure I 7 The open-circuit voltage (Voc) and the short-circuit current (Isc)[22]

Two factors are particularly significant for the real PV and its accompanying circuit. Figure shows, respectively, the open-circuit voltage (V_{oc}) across the terminals when the leads are left unplugged and the short-circuit current (I_{SC}) that flows when the terminals are connected. When the leads of the comparable circuit for the PV cell are shorted together, no current flows in the (real) diode since $V_d = 0$, hence the full current from the ideal source passes via the shorted leads. Since the short-circuit current must be equal to I_{SC}, the size of the ideal current source itself must also be equal to I_{SC}. We can now construct an equation for the equivalent voltage and current. [23, 24]

$$\mathbf{I} = \mathbf{I_{SC}} - \mathbf{I_d} \quad \text{(I.1)}$$

Isc: is the short-circuit current equal to the photo current

$$\mathbf{I} = \mathbf{I_{SC}} - \mathbf{I_0}\left(e^{\frac{qv}{kT}} - \mathbf{1}\right) \quad \text{(I.2)}$$

I: is the current through the diode, (A)

I_0: is the reverse saturation current (a measure of the diode's leakage current) (A)

V: is the applied voltage across the diode (V)

k: is Boltzmann's constant (1.381*10^-23 J/K)

T: is the temperature in Kelvin (K)

q: is the electron charge (1.602*10^-19 C)

It's noteworthy to notice that the second part of equation (I.2) is just an equation for a diode with a negative sign, which implies that the plot of equation (I.2) is exactly Isc summed by the curve I(V) of the shockly reversed diode.

I = 0 and (I.2) for the voltage Voc of the open circuit may be solved when the PV cell's wires are suspended in the air.

$$\mathbf{Voc} = \frac{\mathbf{kT}}{\mathbf{q}}\mathbf{ln}\left(\frac{\mathbf{I_{SC}}}{\mathbf{I_0}} + \mathbf{1}\right) \quad \text{(I.3)}$$

A temperature of 25°C. (I. 2) and (I. 3) becomes:

$$\mathbf{I} = \mathbf{I_{SC}} - \mathbf{I_0}\left(e^{38.9\,v} - \mathbf{1}\right) \quad \text{(I.4)}$$

And:

$$\mathbf{Voc = 0.0257 \ln\left(\frac{I_{SC}}{I_0} + 1\right)} \quad (I.5)$$

Since the short-circuit current I_{SC} in these two equations is precisely proportional to solar irradiation, we can readily display the current versus voltage curve for various solar irradiance levels.

I.3.6 Photovoltaic module (panels):

A photovoltaic module typically consists of an array of photovoltaic cells connected in series and/or parallel to form a larger unit. The series connections of several cells increase the voltage, while paralleling increases the current while maintaining the same voltage. The cells are usually made of silicon, which is a semiconductor material that can absorb photons of light and convert them into electrons. The cells are coated with anti-reflective material to maximize the amount of light that they can absorb, and they are usually encased in a protective layer of glass or plastic.

The electrical output of a photovoltaic module depends on a variety of factors, including the amount of solar irradiation falling on the module, the temperature of the module, and the efficiency of the photovoltaic cells. In general, photovoltaic modules are most efficient at converting solar irradiation into electricity when they are exposed to direct solar irradiation at a moderate temperature. [25]

I.3.6.1 module parameters:

Here is the description of the parameters of a module

The following are some explanations of the variables typically used to describe photovoltaic modules:

- ✓ Open-circuit voltage (Voc): The module's highest voltage when no current is passing through it is known as the open-circuit voltage (Voc). Volts (V) are used to measure it.
- ✓ Short-circuit current (Isc): when the voltage across the module is zero (i.e., when the module is short-circuited), which is the highest that the module is capable of producing. It is expressed in amps (A).
- ✓ Maximum power voltage (Vmp): This refers to the maximum voltage at which a module may generate Usually, it is a little lower than the voltage in an open circuit. Volts (V) are used to measure it.

- ✓ Maximum power current (Imp): The maximum current that the module can output. Usually, it is a little lower than the short-circuit current. It is expressed in amperes (A).
- ✓ MPP (Maximum Power Point): refers to the location on the current-voltage (I-V) curve of a solar panel where the panel outputs its highest amount of electricity. A maximum power point tracking (MPPT) algorithm, which modifies the voltage and current to maintain the panel functioning at its maximum power output, can find and monitor the MPP.
- ✓ PMPP: is the point on the current-voltage (I-V) curve of a solar panel where the panel produces the greatest power. Under standard test circumstances (STC), which are typically 1000 W/m2 of solar irradiation and 25°C for the cell temperature, the maximum amount of electrical power that a solar panel can produce is referred to as the PMPP.
- ✓ Fill factor (FF): This gauge how well a module can produce electricity from solar irradiation that is available. It is the relationship between the module's maximum power output and the sum of the open-circuit voltage and short-circuit current. A percentage is used to represent it. [26]

$$\mathbf{FF} = \frac{\mathbf{P_{max}}}{\mathbf{V_{oc} \times I_{sc}}} = \frac{\mathbf{V_{mp} \times I_{mp}}}{\mathbf{V_{oc} \times I_{sc}}} \qquad (\text{I.6})$$

- ✓ Conversion efficiency η: It is determined by the device's maximum power output to incident light output ratio. It is the energy efficiency of external power conversion. The relationship described below defines it:

$$\boldsymbol{\eta} = \frac{\boldsymbol{P_m}}{\boldsymbol{P_i}} = \frac{\boldsymbol{FF \cdot v_{co} I_{cc}}}{\boldsymbol{P_i}} \qquad (\text{I.7})$$

I.4 MODÈLE MATHÉMATIQUE D'UNE CELLULE SOLAIRE :

The mathematical model of a solar cell is a mathematical equation that describes the relationship between the current, voltage, and power output of the solar cell under different operating conditions The most commonly used mathematical model for a solar cell is the single-diode model (**Figure I.8**):

- ➢ Current source: Models the conversion of luminous flux into electric current
- ➢ A diode: Models the PN junction

- A series resistance Rs: Models the various resistances of the different layers of the cell
- A parallel resistor Rsh: Characterizes the leakage current in the diode and edge effects of the junction.

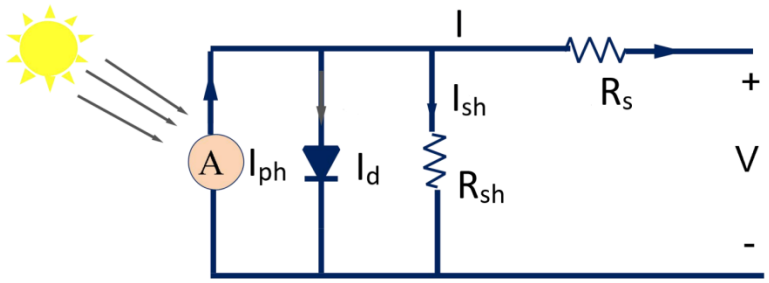

Figure I 8 equivalent circuit scheme for an organic solar cell[27]

which is based on the following equation:

$$\boldsymbol{I = I_{ph} - I_{sh} - I_d} \quad \text{(I.8)}$$

Or:

$$\boldsymbol{I(V) = I_{ph} - \frac{V+I.R_s}{R_{sh}} - I_0\left[e^{\left(\frac{q(V+I.R_s)}{nKT}\right)} - 1\right]} \quad \text{(I.9)}$$

With:

I: current output of the solar cell

R_s: series resistance of the solar cell

n: ideality factor (1<n< 2)

R_{sh}: shunt resistance of the solar cell

The generated photo current I_{ph} depends on the illumination and the temperature, it is expressed as follows

$$\boldsymbol{I_{ph} = I_{cref} \times (G/G_{STS})} \quad \text{(I.10)}$$

I_{cref}: is the reference current, which is the current generated by the solar cell when it is illuminated with light of intensity GSTS

G/G_{STS}: is called the relative intensity factor, which is a dimensionless quantity that represents the ratio of the actual light intensity to the reference light intensity

The temperature, the material's prohibited band width, and the number of cells in series all affect the saturation current. It comes from:

$$\mathbf{I} = \frac{\mathbf{Icref}}{\mathbf{e}^{\left(\frac{\mathbf{Voc}}{\mathbf{V1}}\right)-1}} \times \left[\frac{\mathbf{T}}{\mathbf{T0}}\right]^{\mathbf{3}} \times \mathbf{e}^{\left(\frac{-\mathbf{qEg}}{\mathbf{KT}}\right)} \quad \text{(I.11)}$$

provided that a photovoltaic generator is composed of series-parallel arrays of photovoltaic cells and equation (I.9), the relationship between a GPV's current and voltage is provided by

$$\boldsymbol{I(V) = I_{ph}.\,Np - Np.\,I_0\left[e^{\left(\frac{q(V+I.R_S)}{Ns.nKT}\right)} - 1\right] - \frac{V+I.R_s}{R_{sh}}} \qquad \text{(I.12)}$$

With:

N_s: Number of cells in series.

N_p: Number of cells in parallel.

The following figure provides the electric model of the solar generator:

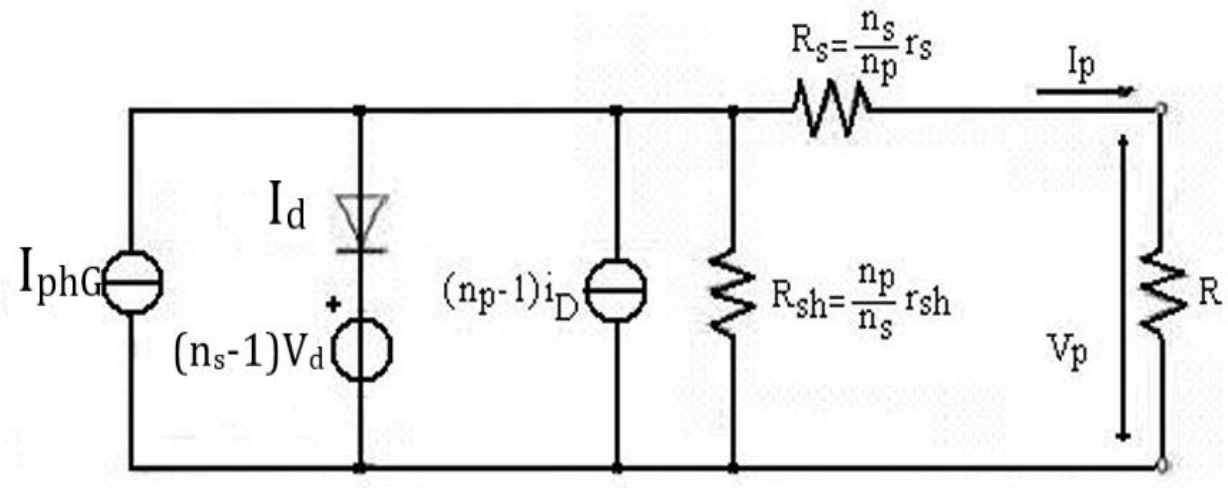

Figure I 9 Model and equivalent Scheme of a photovoltaic generator using the single exponential model[28]

I.5 SIMULATION OF A PHOTOVOLTAIC CELL:

I.5.1 Characteristics I (V) and P (V):

Figures (I.10) and (I.11) depict the outcomes of a simulation of the current-voltage I(V) and power-voltage P(V) characteristics of the solar cell under standard circumstances (T = 25 °C, G = 1000 W/m2) using MATLAB software: The current-voltage characteristic of a solar cell at G = 1000 W/m2 and T = 25 °C is shown in Figure (I.10)

We used these formulas to create these curves:

$$\boldsymbol{P = I * V} \qquad \text{(I.13)}$$

P: the power (w)

And we used

$$\mathbf{I} = \mathbf{I_{SC}} - \mathbf{I_0}\left(e^{\frac{qv}{kT}} - \mathbf{1}\right) \quad \text{(I.14)}$$

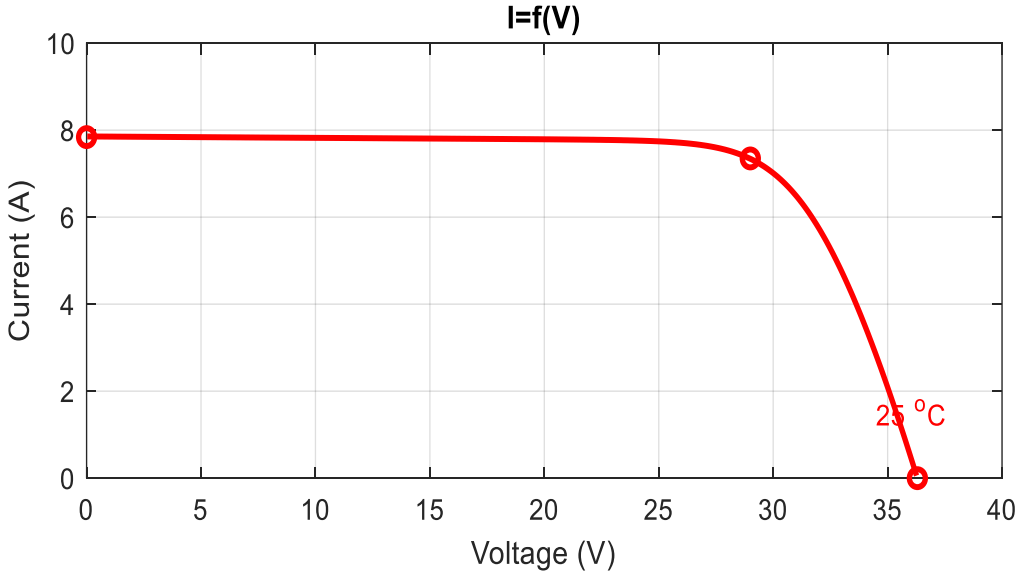

Figure I 10 I(V) characteristic of a cell (T=25°C, G=1000W/m²)

The connection between a photovoltaic cell's output voltage and current is known as its I (V) characteristic. It offers crucial details on the cell's performance and efficiency and is a visual depiction of the current-voltage behavior of the cell. A solar cell's I (V) curve typically has a nonlinear form and shows a maximum power point where the sum of the current and voltage is highest.

The power-voltage characteristics of a solar cell at G=1000 W/m2 and T=25 °C are shown in figure (I.11). The maximum power is P max=213.15W

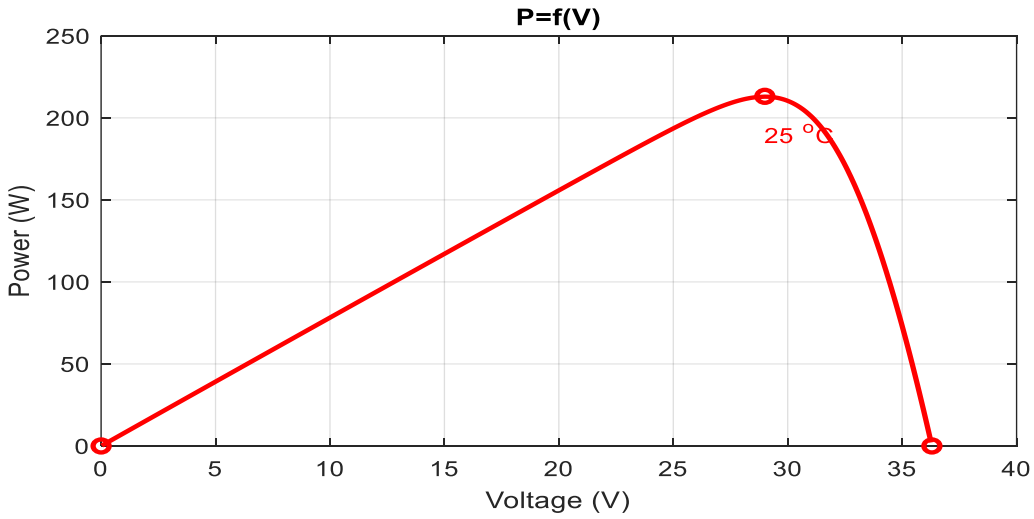

Figure I 11 P(V) characteristic of a cell (T=25°C, G=1000W/m²)

When the voltage increases, the power output of a photovoltaic cell also increases up to a certain point called the maximum power point (Pmax), where the product of the voltage

and current is at its highest. However, if the voltage continues to increase beyond the maximum power point, the cell's efficiency and power output decrease due to the increased losses and decreased current flow. This leads to a decline in the I(V) curve after the maximum power point.

I.5.2 Serial and parallel association of PV modules:

I.5.2.1 Association of cells in parallel:

When n cells are linked in parallel the voltage applied to each cell is the same and the current increases in direct proportion to the number of parallel modules.

$$U = U1 = U2 \ldots\ldots = Un \quad \text{(I.15)}$$

$$I = I1 + I2 \ \ldots\ldots + In \quad \text{(I.16)}$$

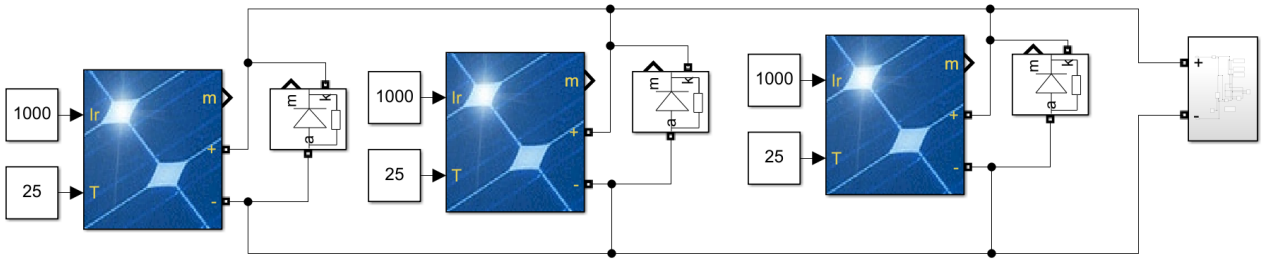

Figure I 12 Simulink diagram of three solar modules in parallel

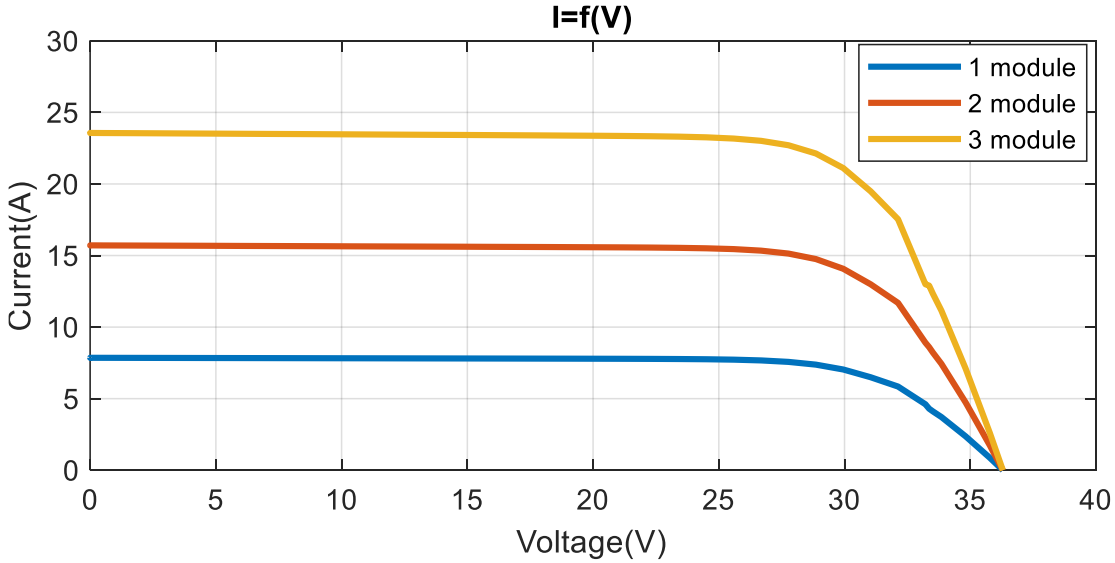

Figure I 13 Resultant I-V characteristics of an array of three modules in parallel

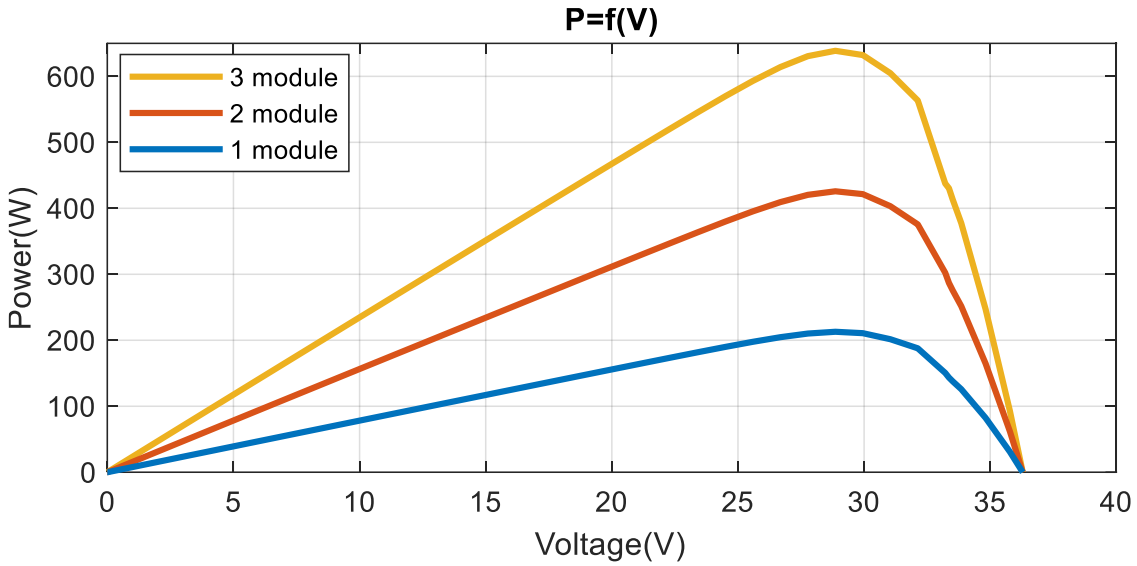

Figure I 14 Resultant P-V characteristics of an array of three modules in parallel

I.5.2.2 Association of cells in series:

When n cells are linked in series the current applied to each cell is the same and the voltage increases in direct proportion to the number of series modules.

$$U = U1 + U2 \ldots\ldots + Un \quad \text{(I.17)}$$

$$I = I1 = I2 \ldots\ldots = In \quad \text{(I.18)}$$

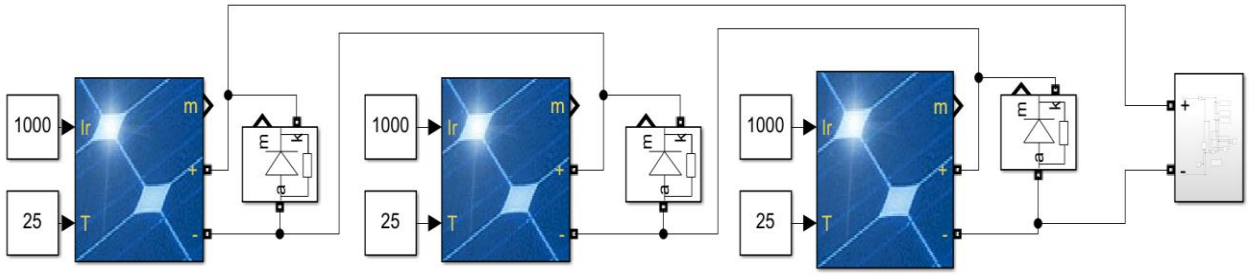

Figure I 15 Simulink diagram of three solar modules in series

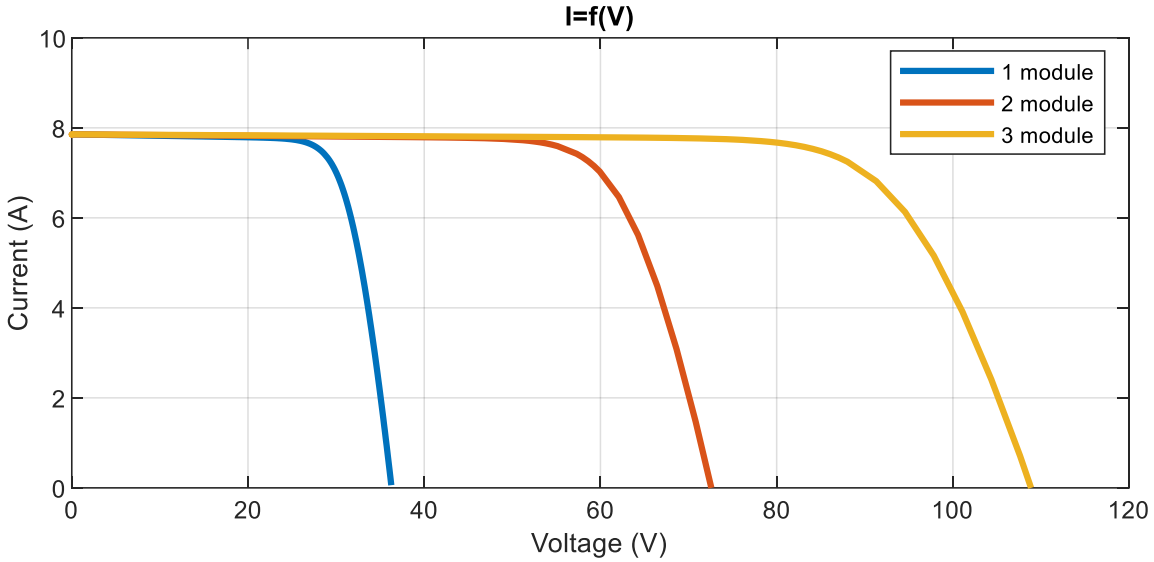

Figure I 16 Resultant I-V characteristics of an array of three modules in series

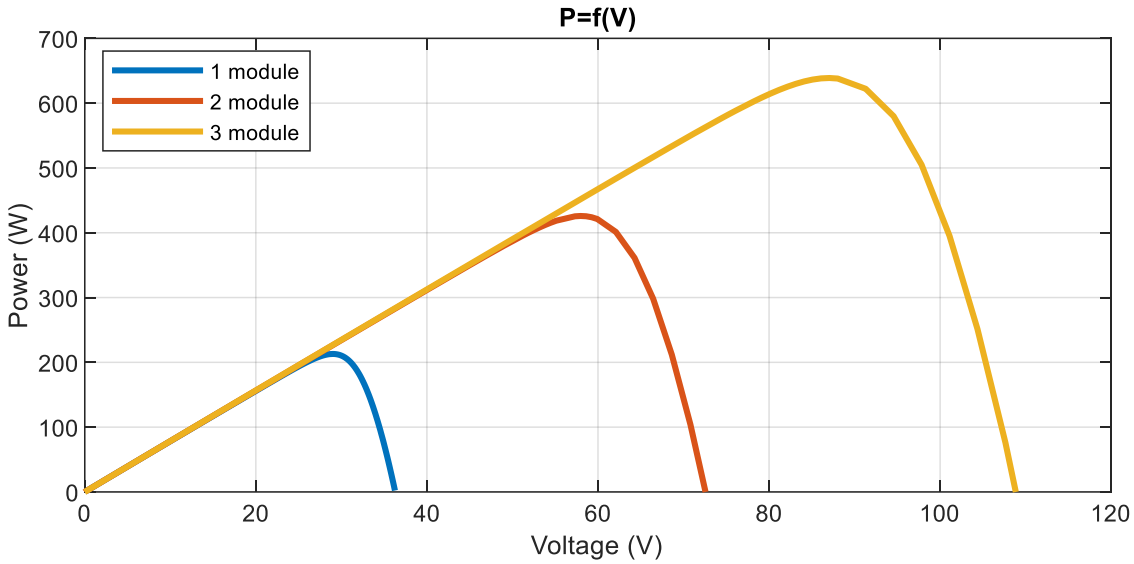

Figure I 17 Resultant P-V characteristics of an array of three modules in series

I.5.3 Climatic effects on the PV cell:

Les cellules photovoltaïques sont sensibles aux conditions climatiques. Voici quelques-uns des effets climatiques qui peuvent avoir un impact sur la performance des cellules PV :

I.5.3.1 Temperature:

The efficiency of photovoltaic cells decreases with increasing temperature. This is due to the effect of heat on the electrons in the cell, which can reduce the open circuit voltage (Voc) and maximum power (Pmax). [29]

The two figures (I.18) and (I.19)) represent graphing using MATLAB the current I(V) and power P(V) characteristics under the same illuminance condition (G=1000 W/m²) and for different temperatures (T=0, 25, 50 ,75)

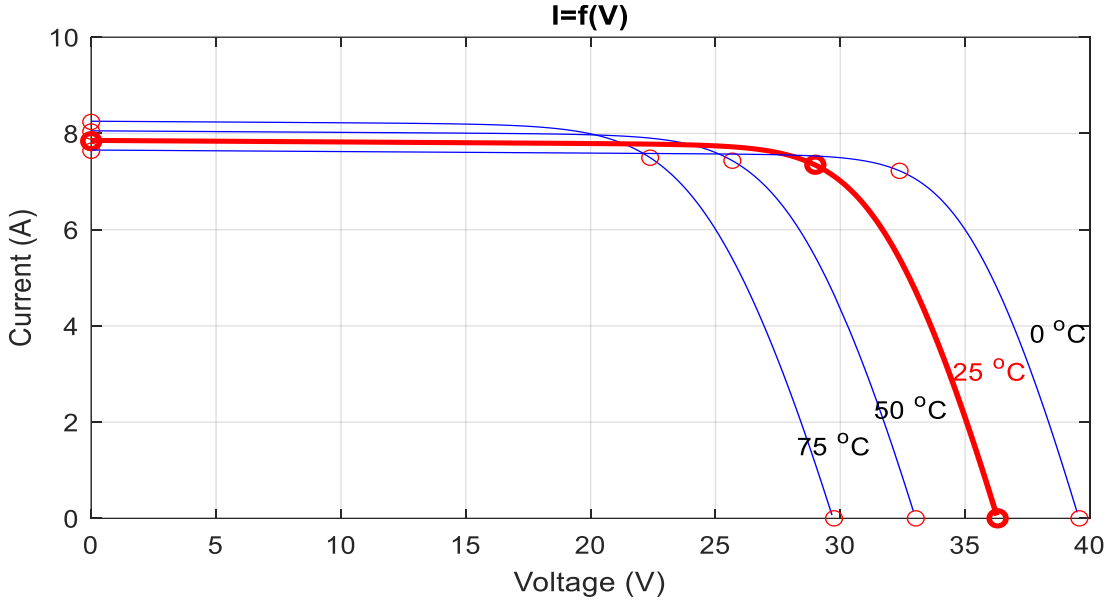

Figure I 18 Characteristic I(V) for different temperatures (G=1000W/m²)

We see that when the temperature rises, the voltage across the open circuit falls, but it slightly increases across the short circuit.

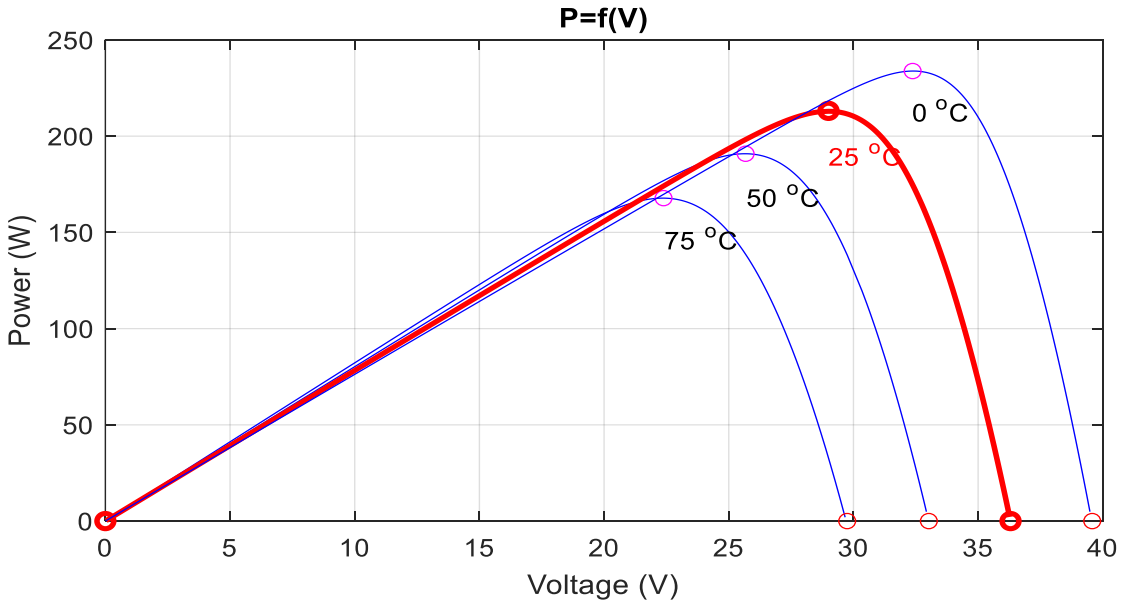

Figure I 19 Characteristic P(V) for different temperatures (G=1000W/m²)

It has been shown that when temperature rises, maximum power drops. We really discover that temperature has a detrimental impact on open circuit voltage. Therefore, we can conclude as follows:

PV cells work better in a chilly climate with a clear sky.

I.5.3.2 Solar Irradiation:

The amount of solar irradiation available can have a significant impact on the performance of PV cells. Adverse weather conditions, such as clouds or rain, can reduce the amount of solar irradiation reaching the cell, reducing energy production. [29]

The two figures (I.20) and (I.21) represent graphing using MATLAB the characteristics (I-V) and (P-V) of a cell as a function of the variation in illumination (G = 250,500,750,1000 W/m2) at a temperature constant (T = 25 °C)

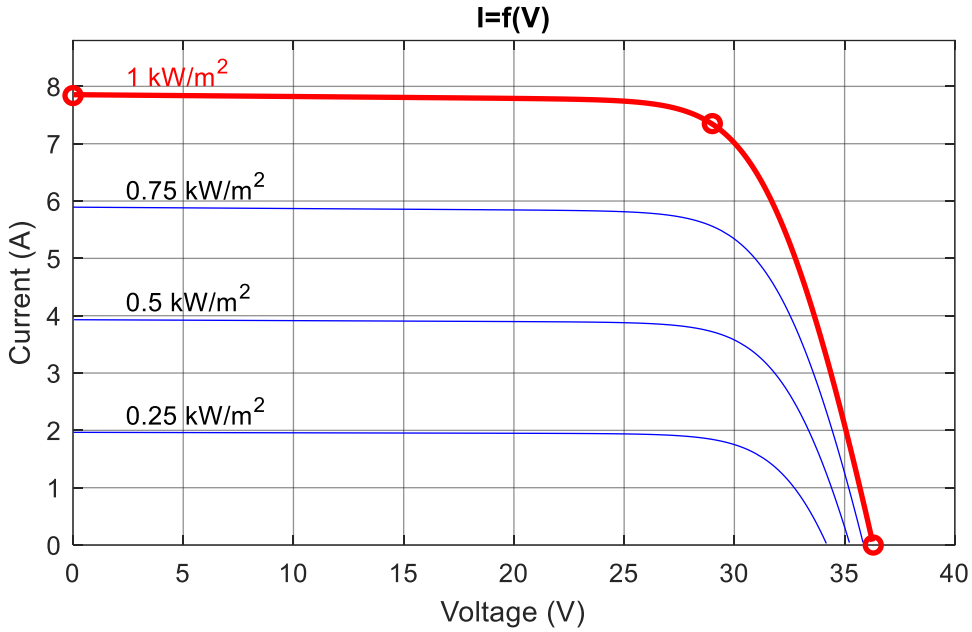

Figure I 20 Characteristic I(V) for different levels of illumination (T=25°C)

The incident irradiation has a direct proportional relationship with the short-circuit current. However, the tension very slightly changes, as seen by the lighting picture (I.20).

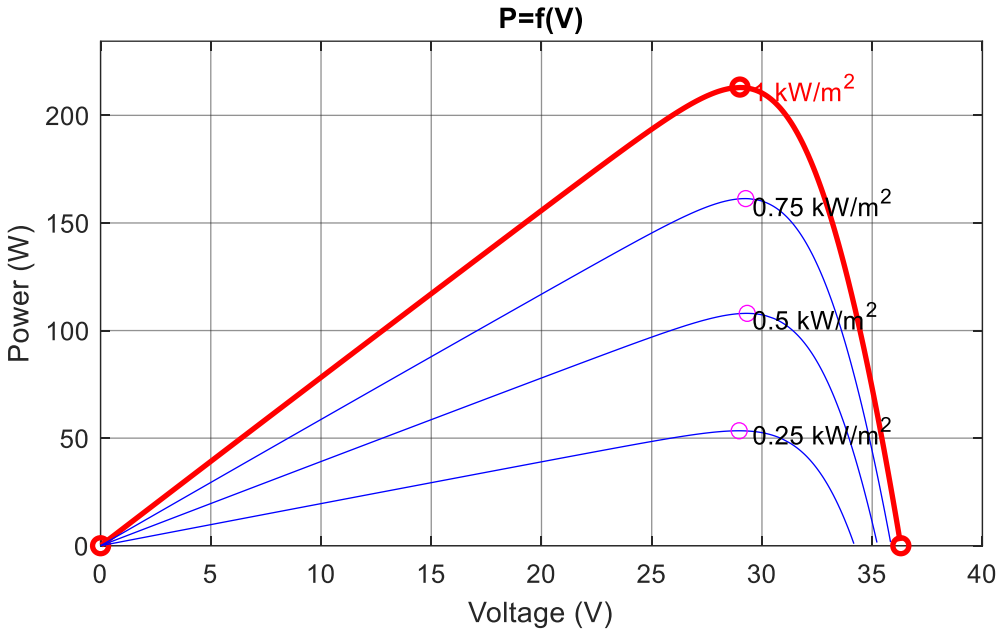

Figure I 21 Characteristic P(V) for different levels of illumination (T=25°C)

Figure (I.21) shows how the power output of the cell varies with voltage for various degrees of illumination, allowing us to infer the impact of lighting on the P(V) characteristic.

It has been shown that when light levels rise, the maximum power rises as well. As can be observed, the open circuit voltage is positively impacted by illumination.

I.5.3.3 Humidity:

High humidity can affect the performance of photovoltaic cells. High humidity can corrode electrical connections and reduce cell life[30].

I.5.3.4 Wind:

Strong winds can physically damage PV cells. Additionally, winds that can kick up dust and debris can reduce the amount of solar irradiation reaching the cell. [30]

I.6 ADVANTAGES AND DISADVANTAGES OF PHOTOVOLTAIC SYSTEMS:

Advantages of Photovoltaic Systems:

- ✓ Renewable Energy: Unlike fossil fuels, which are limited and non-renewable, solar energy, which is used by PV systems, is renewable and sustainable.
- ✓ Low Maintenance: PV systems require less maintenance since they have few moving components and are simple to use. They merely need to be cleaned occasionally to get rid of dust and grime.

- ✓ Long Lifespan: Most PV panels endure 25 to 30 years or more, making them a long-lasting component of PV systems.
- ✓ Quiet Operation: PV systems operate quietly, making them perfect for residential settings where noise pollution is a problem.
- ✓ Energy Independence: PV systems enable energy independence, decreasing dependency on conventional energy sources and carbon emissions. [31]

Disadvantages of Photovoltaic systems:

- ✓ High Initial Cost: The initial cost of a PV system can be high, including the cost of installation and equipment.
- ✓ Weather dependent: PV systems depend on solar irradiation to generate power, and weather variations like clouds or shade can have an impact on their production.
- ✓ Space Needed: PV systems need room to be installed, and they also need a lot of space to produce enough energy to power a house or a company.
- ✓ Limited Efficiency: The greatest efficiency of PV systems which convert solar irradiation into electricity is presently approximately 20%.
- ✓ Environmental Impact: The manufacture of hazardous chemicals and the disposal of PV panels might have an adverse effect on the environment. [32]

I.7 CONCLUSION:

This chapter provides an introduction to renewable energies, with a focus on photovoltaic solar energy. It includes a general overview of photovoltaic systems, covering solar irradiation, photovoltaic conversion. We discuss various PV cell technologies, modeling approaches, In the final part, we discussed the effects of heat and solar irradiation on photovoltaic cells and the pros and cons of photovoltaic systems

II)CHAPITRE II: Study and comparison of the different configurations of photovoltaic panels under the effect of partial shade

II.1 INTRODUCTION:

The performance of a photovoltaic module can be significantly compromised, not only in comparison to its maximum power point but also under typical weather conditions. This is due to several factors, including shading and temperature, which can adversely affect the electricity production of a photovoltaic (PV) panel.

Partial shading (PS) is a common issue that can greatly affect the performance of solar photovoltaic (PV) panels. This occurs when some parts of a PV array are shaded, which can be caused by various obstructions such as buildings, trees, or even cloud cover. When a portion of the PV array is shaded, the shaded modules cannot produce as much current as the unshaded ones since all the modules are typically connected in series and/or in parallel. As a result, the entire PV system's output can be reduced, sometimes significantly. When a photovoltaic system is partially shaded, the shaded units can negatively affect the unshaded units, causing a decrease in voltage and a loss of energy. Shaded units may also act as a load, dissipating energy as heat and causing hot spots. This problem has been the subject of research in recent years, and various techniques have been proposed to mitigate its effects. These solutions aim to minimize the impact of shading on PV panels and improve their overall performance.

In this chapter, we study different configurations of photovoltaic systems to achieve the required voltages and currents. These configurations include Serial-Parallel (SP), Total-Cross-Tied (TCT), Bridge Linked (BL), and Honey Comb (HC).

II.2 Effect of shading:

There are two different kinds of shading that operate at different levels: the module level and the cell level and They are referred to as homogenous shading impacting the module and partial shading affecting one cell.

II.2.1 Homogeneous shading:

In this case, the distribution of the inciting illumination is homogeneous over the entire surface of the cell or photovoltaic module. We carried out a test on a panel of 60 cells by varying the illumination from 1000 W/m2 to 250 W/m2. Figure Il.1 and Figure II.2 represents the variation of the I-V and P-V characteristic when the 60 cells are occulted in a homogeneous manner. The chain behaves as if the global illumination had been reduced.

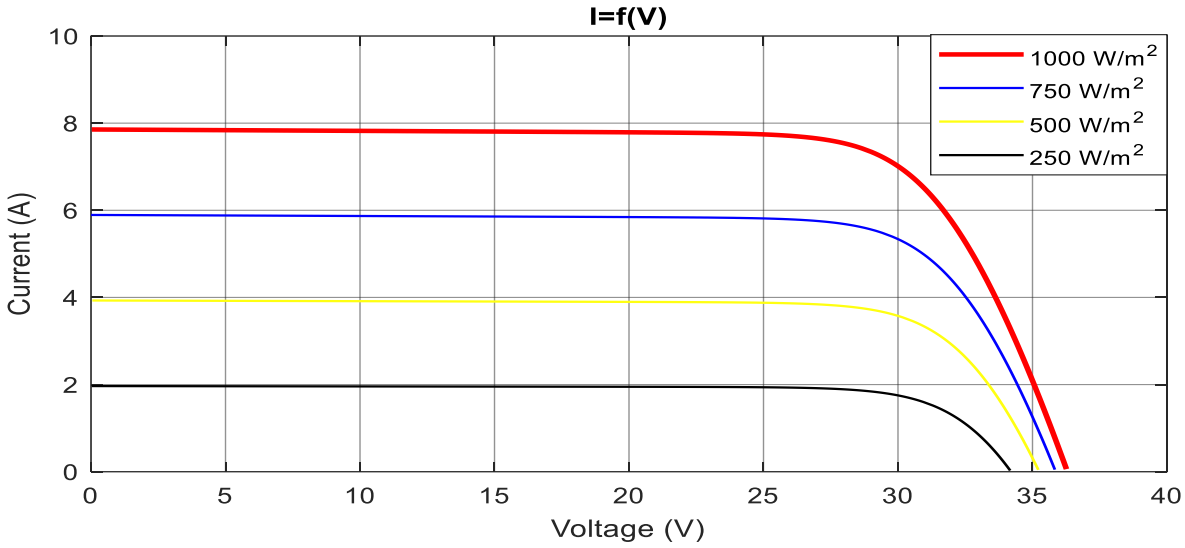

Figure II 1 I=f(V) of a panel under different illuminations

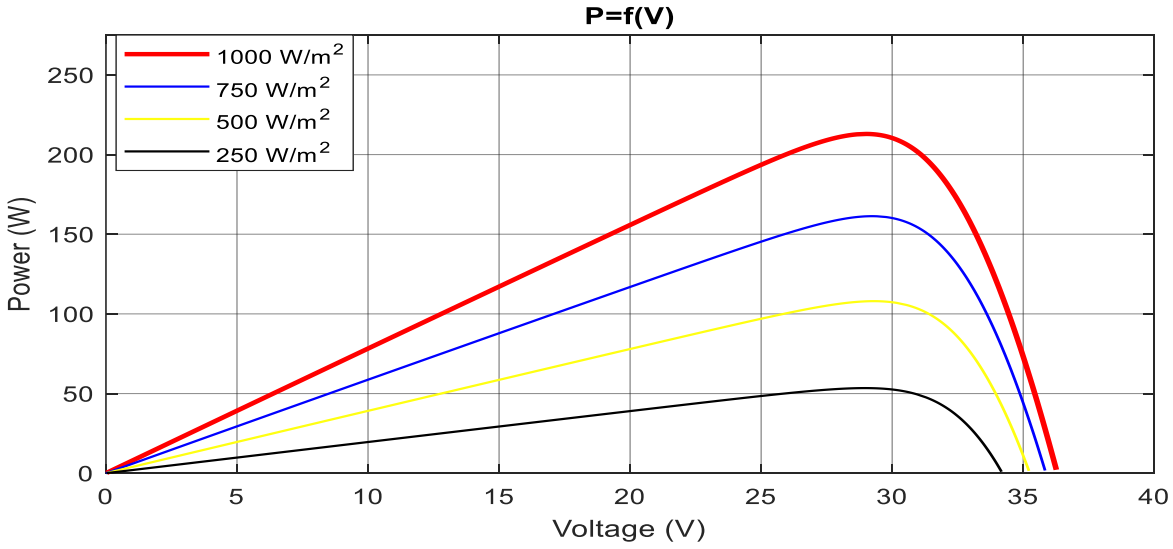

Figure II 2 P=f(V) characteristic of a panel under different illuminations

II.2.2 Inhomogeneous shading (partial):

In this case, the distribution of the inciting illumination is not homogeneous over the entire surface of the cell or the photovoltaic module the cells receive different illuminations of less than 1000 W/m².

II.2.2.1 Test 1:

To carry out this test, we put 4 cells in series under different illuminations, for the first cell G1= 1000 W/m², for the second cell G2= 750 W/m² and for the third cell G3= 500 W/ m² and for the fourth cell G4= 250 W/m²

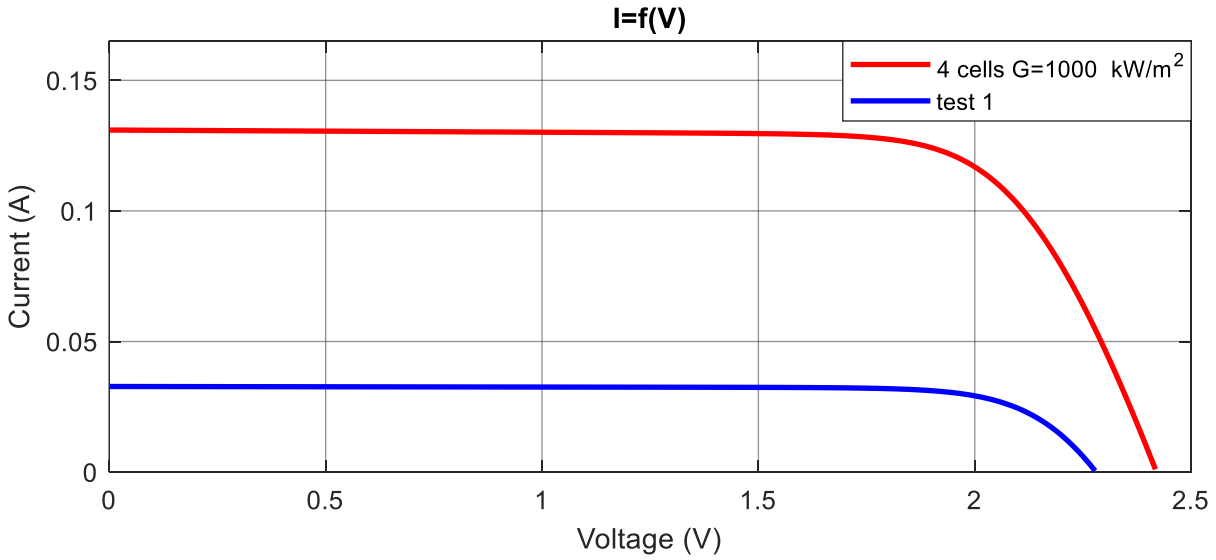

Figure II 3 I-V of a chain of 4 cells of which one cell is shaded at 25% and at 50% and at 75%

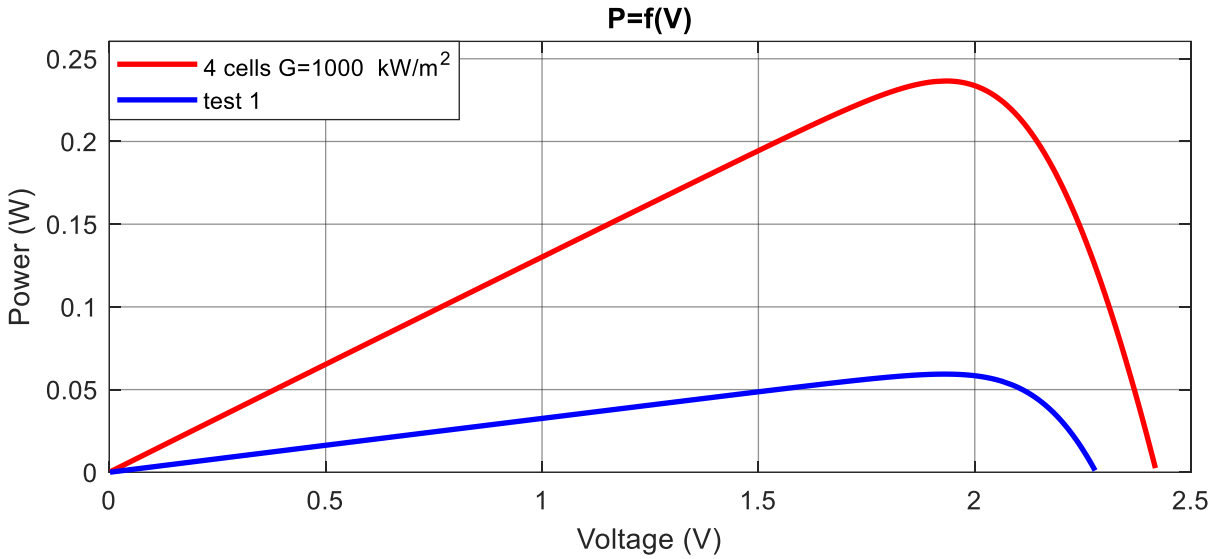

Figure II 4 P-V of a chain of 4 cells of which one cell is shaded at 25% and at 50% and at 75%

II.2.2.2 Test2:

To carry out this test, 4 cells are placed in series, for the first and the second and the third cell G= 1000 W/m² and for the fourth cell G= 100 W/m².

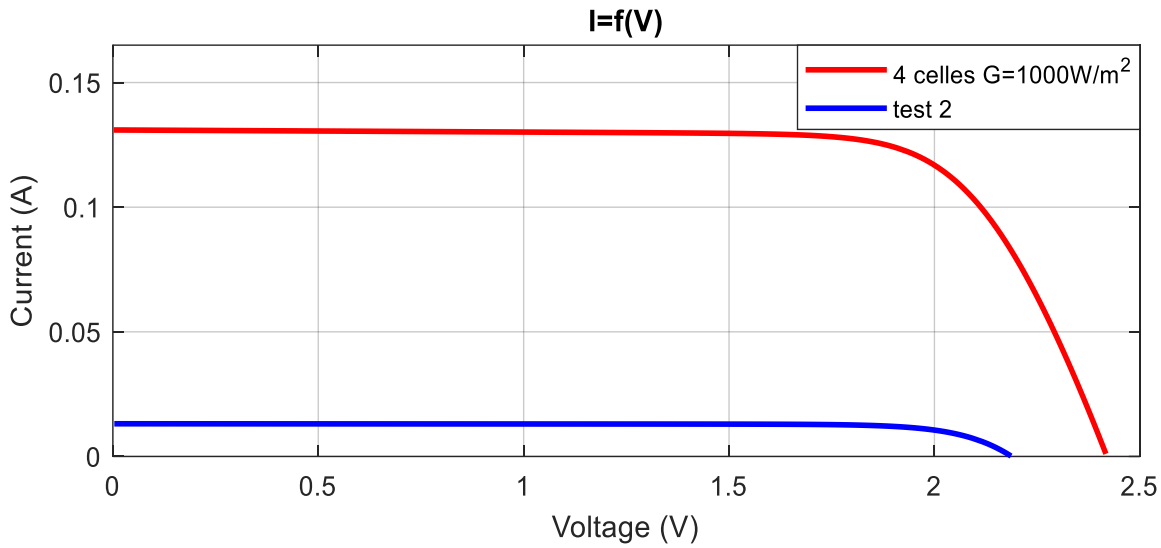

Figure II 5 shows the I-V characteristics of a chain of four cells, with one cell shaded at 90%

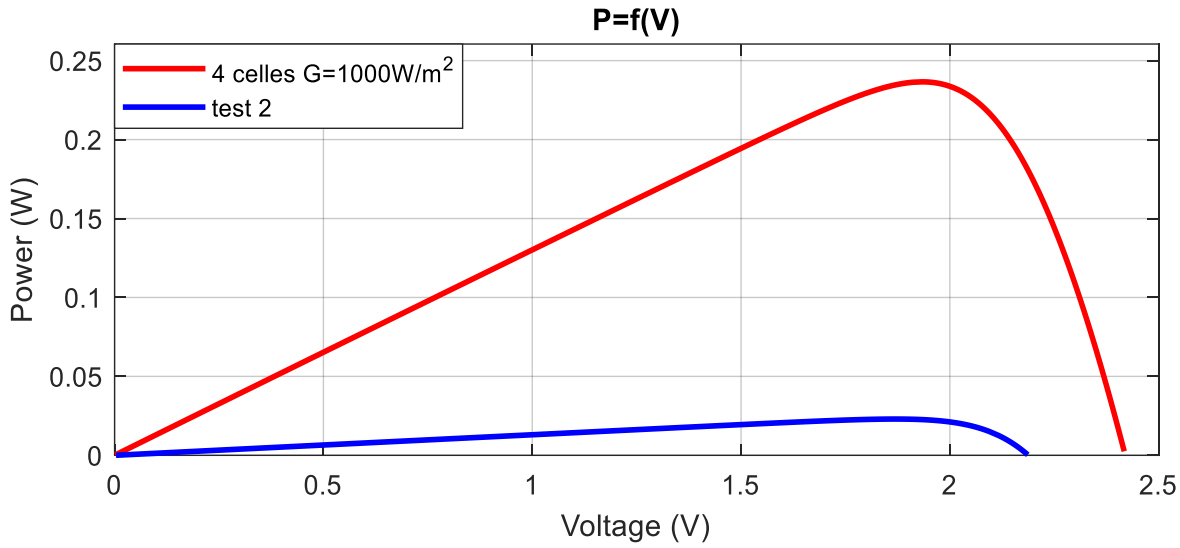

Figure II 6 shows the P-V characteristics of a chain of four cells, with one cell shaded at 90%.

II.2.2.3 Test 3:

For this test, we lined up four panels in series G1 = 1000 W/m2 for the first panel G2 = 750 W/m2 for the second and G3 = 500 W/m2 for the third G4=250W/m2 for the fourth cell

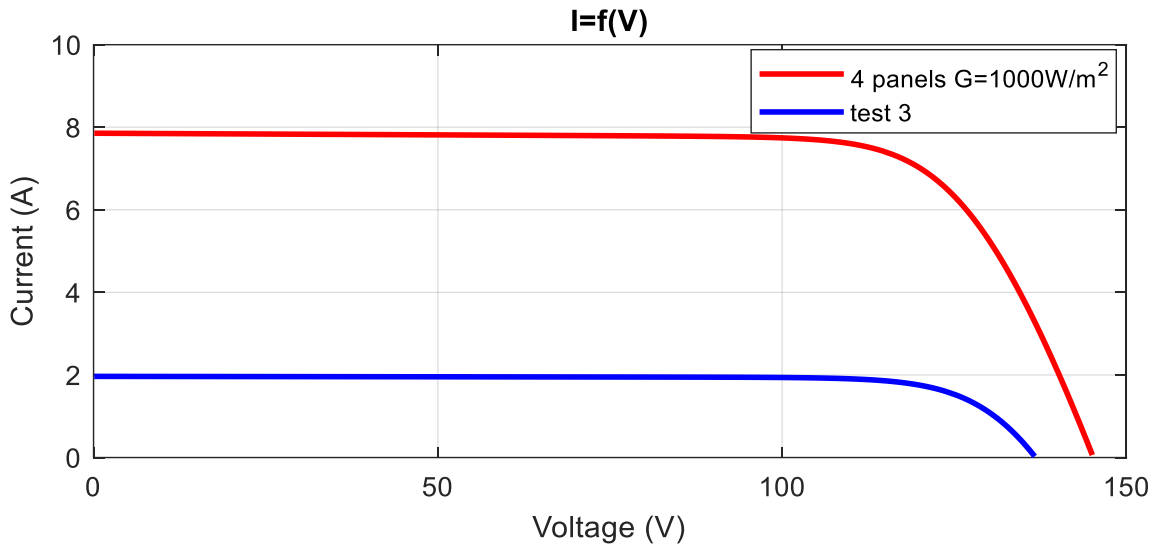

Figure II 7 shows the I-V characteristic of 4 PV panels in series under partial shade (1000, 750, 500,250 W/m²) without diode

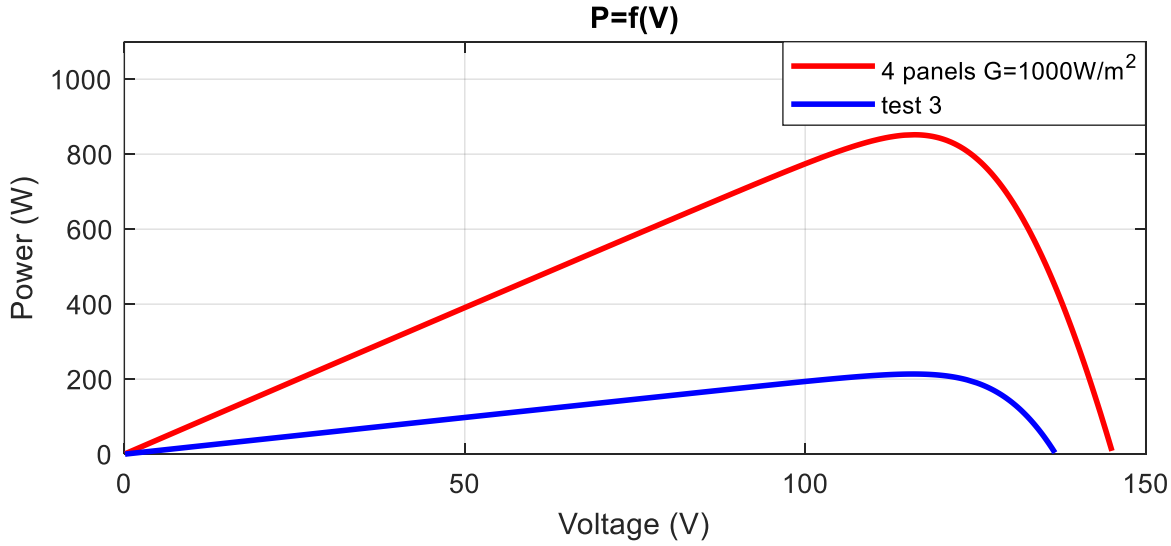

Figure II 8 shows the P-V characteristic of 4 PV panels in series under partial shade (1000, 750, 500,250 W/m²) without diode

It is evident by examining the electrical properties of the solar panel under various shadowing scenarios (Figures II.3 to Figure II.8) that there is a significant reduction in the current and power output of the panel.

Therefore, in order not to risk compromising the profitability of a photovoltaic installation, it is necessary, from the planning phase, to minimize the losses of yield due to shading conditions. Use of bypass diodes which are diodes positioned in anti-parallel with each cell or a group of cells, is one of the solutions.

II.3 Hotspots:

Destructive malfunctions related to the connection of cells and their work in the shadow state should be avoided in order to extend the life of the unit. The series connection of the solar panel's cells ensures that the current going through each cell is the same. This implies that IF a cell in the series is shaded, it obstructs the passage of current, causing the cell to overheat and sustain damage. This phenomenon is referred to as a "hot spot".[33]

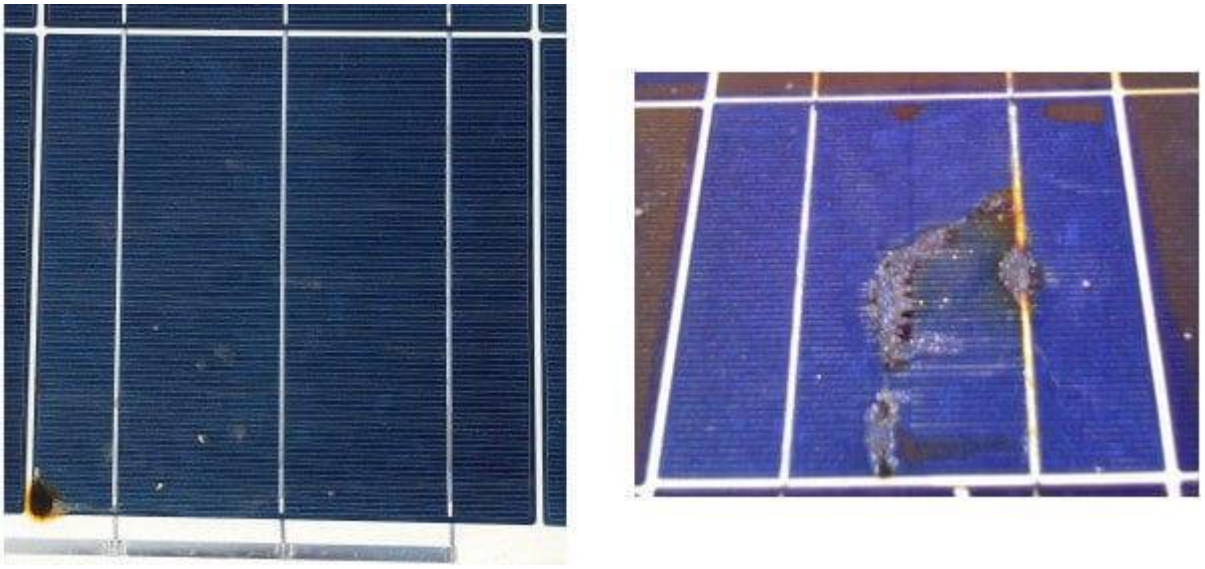

Figure II 9 Examples of two separate types of hot spot-related cell damage[34]

II.4 bypass diode:

In photovoltaic (PV) systems, a bypass diode is a part that guards against harm to the PV cells It is connected in parallel with each PV cell or module and allows current to flow around a cell or module that is shaded or damaged, preventing the entire system from being affected. When a cell or module is damaged or shaded it can become a load on the rest of the system which might lead to overheating and eventual system failure. The bypass diode provides an alternate path for the current to flow, bypassing the shaded or damaged cell or module. [35, 36]

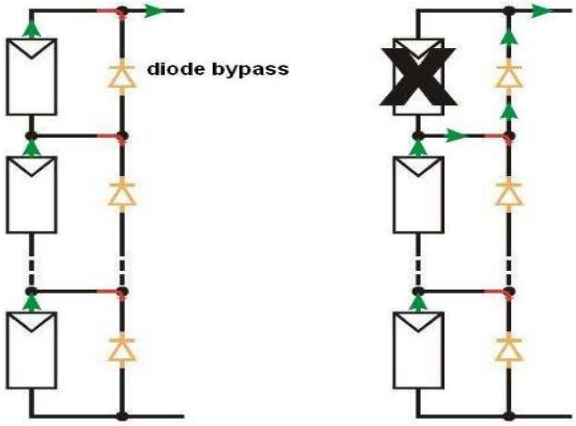

Figure II 10 Architecture of a photovoltaic panel design includes bypass diode activation when a cell fails[37]

The series diode: which is positioned between the battery and the module, stops current from returning to the module while it is dark. It is also known as an anti-return diode in this instance. When a battery provides the load, this diode is necessary to prevent the PV module from charging overnight.

II.4.1.1 Test 4:

We repeated test 1 to conduct this test, but this time we used four cells in series and parallel bypass diodes under various lighting conditions

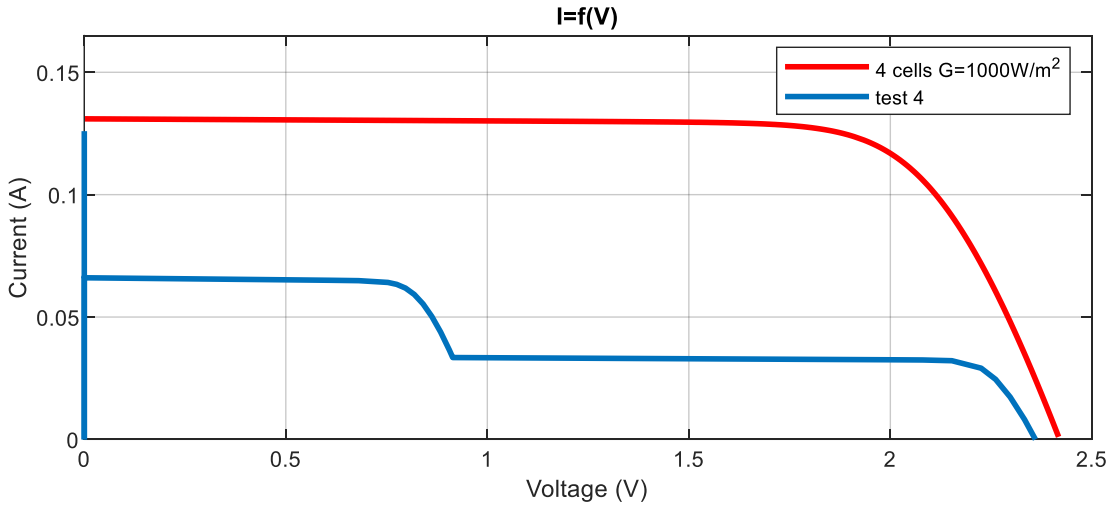

Figure II 11 I-V of a series of (4 cells white diode bypass) of which one cell is shaded at 25% and at 50% and at 75%

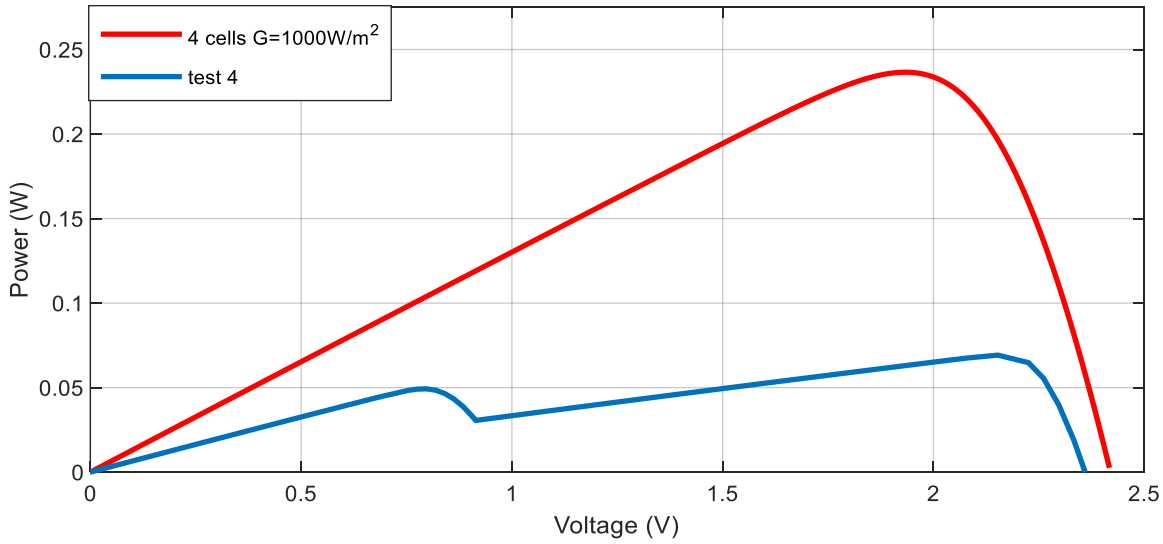

Figure II 12 P-V of a series of (4 cells white diode bypass) of which one cell is shaded at 25% and at 50% and at 75%

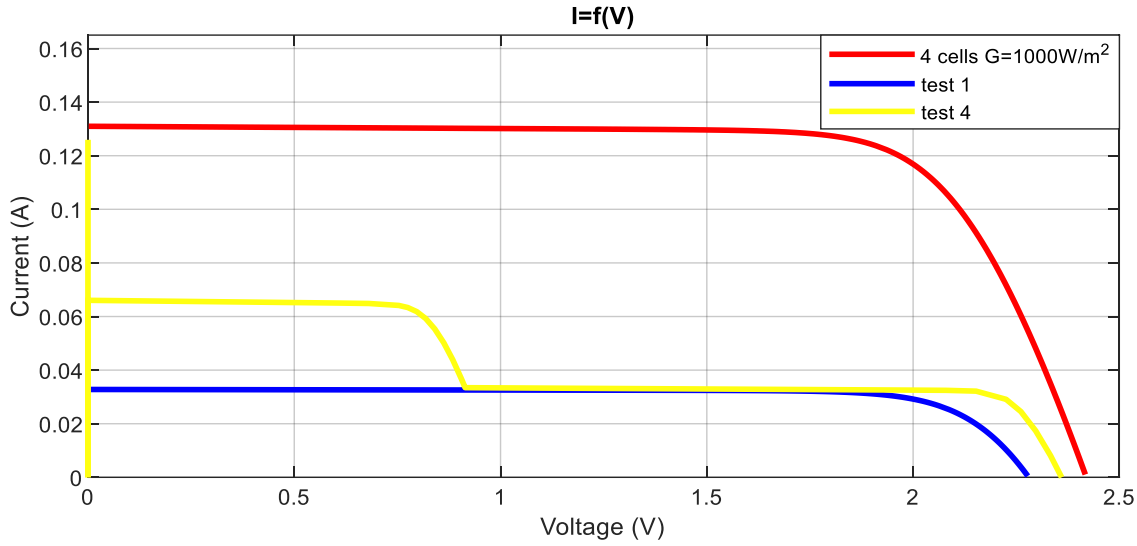

Figure II 13 Effect of the bypass diode on the I-V characteristic of a module PV

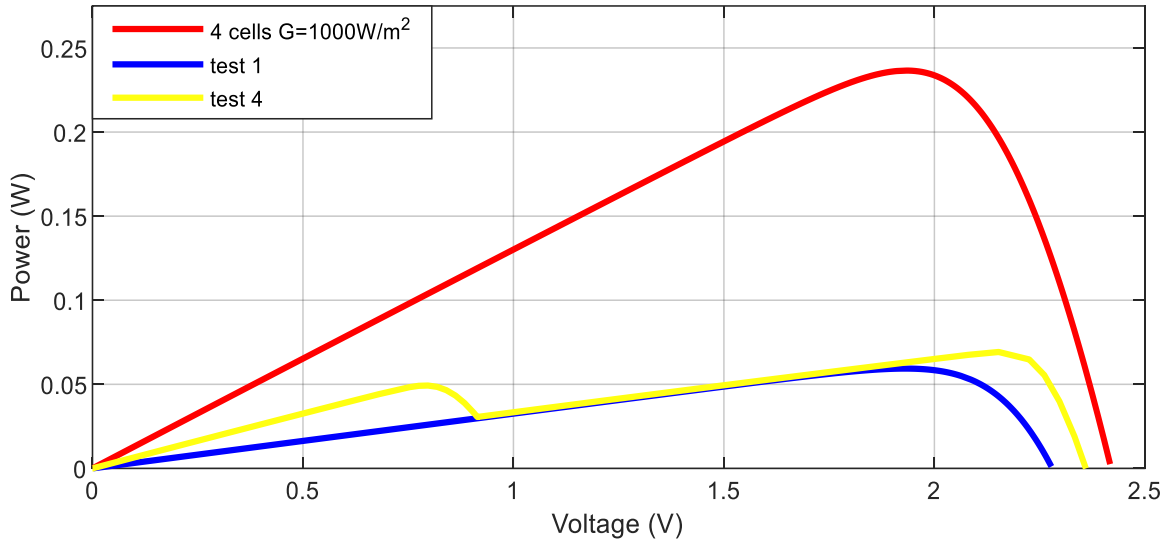

Figure II 14 Effect of the bypass diode on the P-V characteristic of a module PV

II.4.1.2 Test 5:

This test is run on a string of three cells, one of which has a bypass diode shading it 90% of the time.

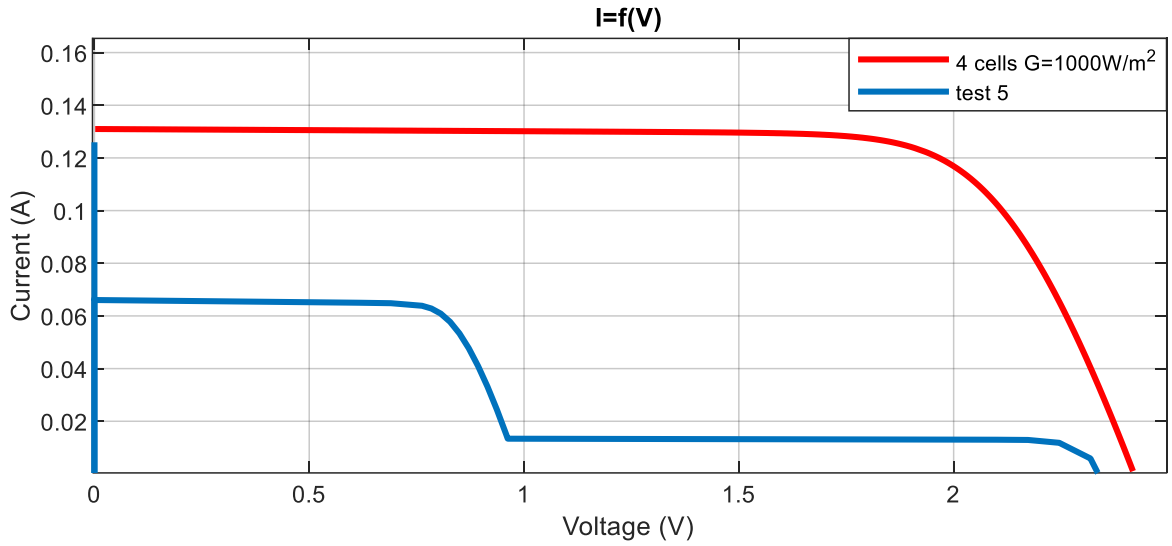

Figure II 15 shows the I-V characteristics of a series of four cells Figure white diode bypass with one cell shaded at 90%.

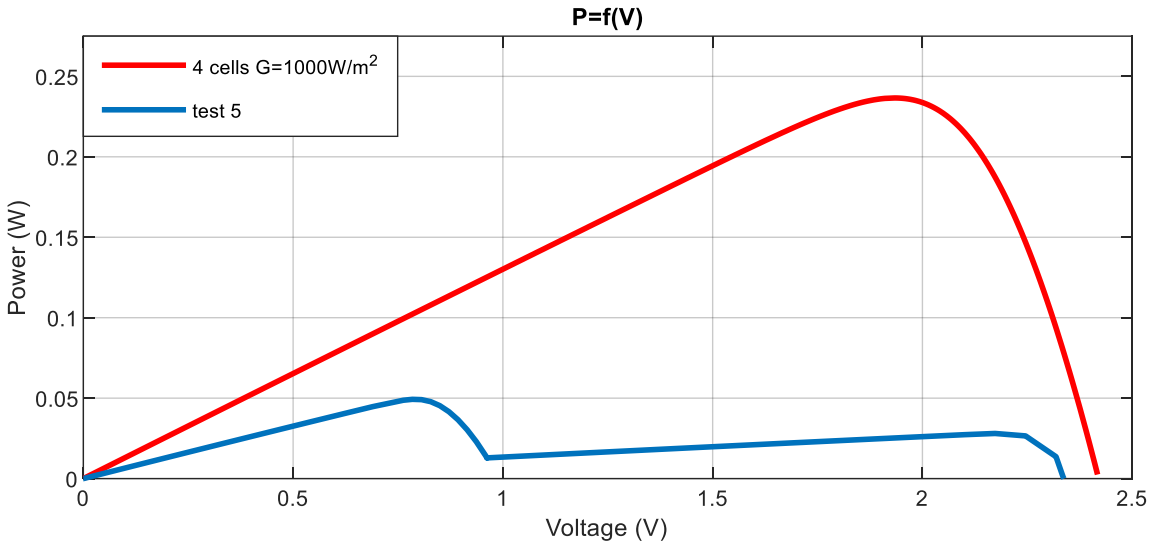

Figure II 16 shows the I-V characteristics of a chain of four cells Figure white diode bypass, with one cell shaded at 90%

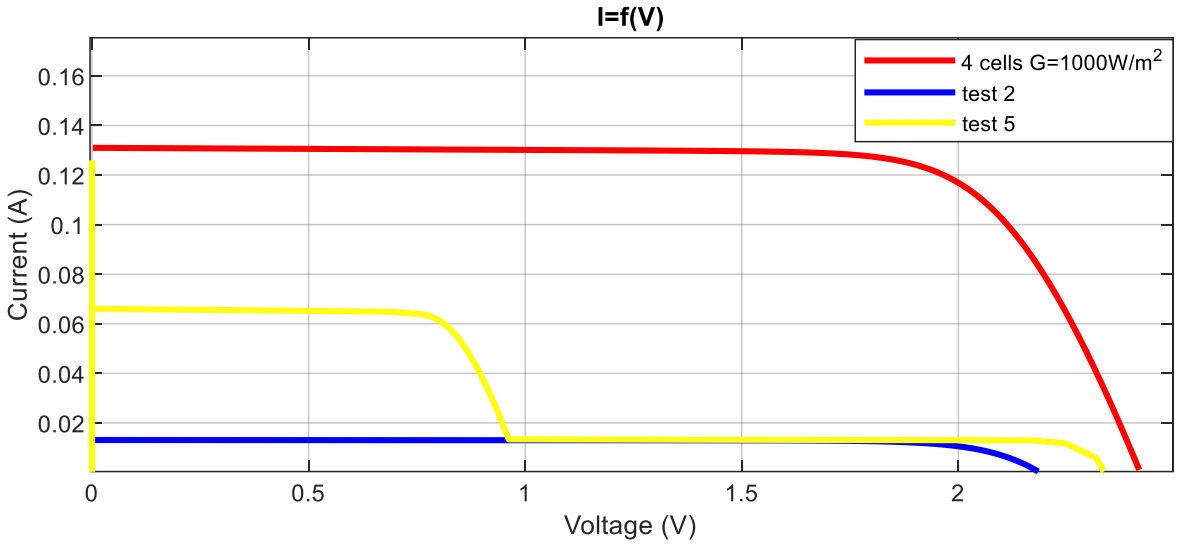

Figure II 17 I-V characteristic of 4 PV cells in series under partial shade (1000,750,500,100 W/m²) with and without diode

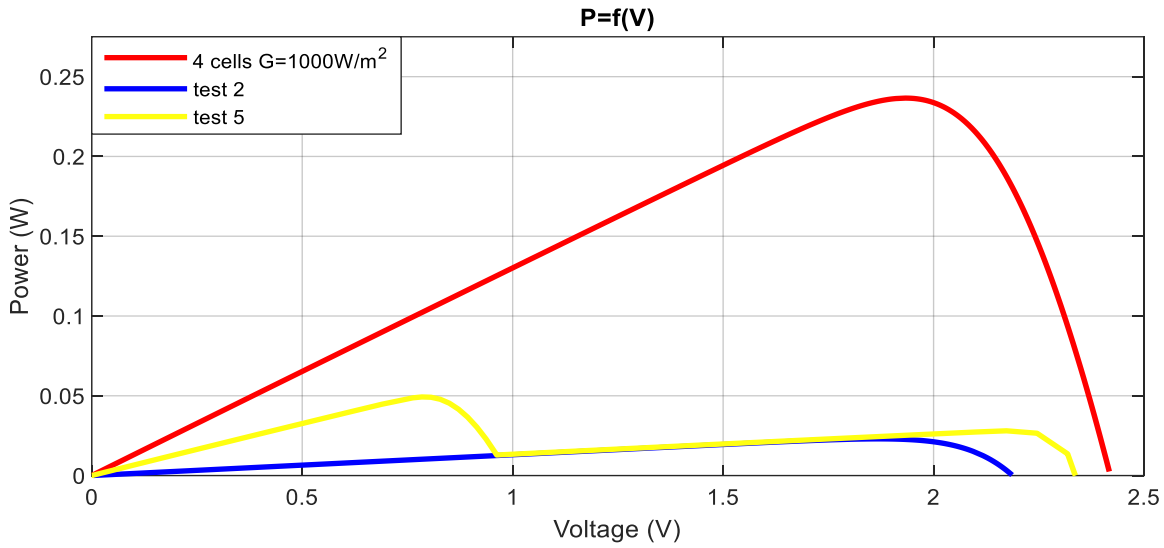

Figure II 18 P-V characteristic of 4 PV cells in series under partial shade (1000,750,500,100 W/m²) with and without diode

II.4.1.3 Test 6:

In this test, a bypass diode is connected in parallel with a set of cells equivalent to a module. In this scenario, G1 = 1000 W/m2, G2 = 750 W/m2, G3 = 500 W/m2, and G4 = 250 W/m2.

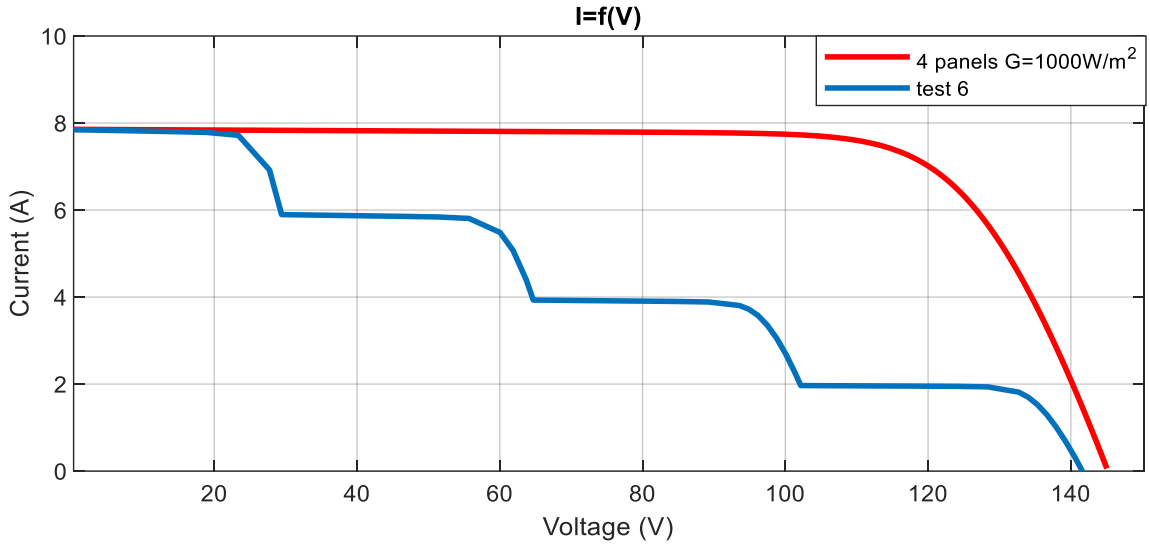

Figure II 19 Characteristic I-V of four parallel PV panels with partial shading (1000, 750,500, and 250 W/m2) with a diode

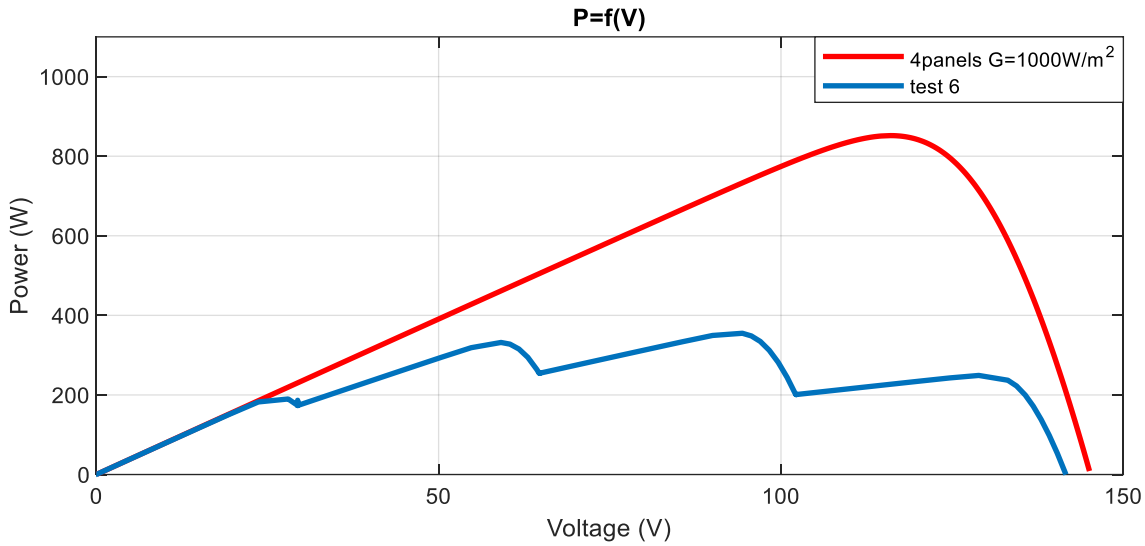

Figure II 20 Characteristic P-V of four parallel PV panels with partial shading (1000, 750,500, and 250 W/m2) with a diode

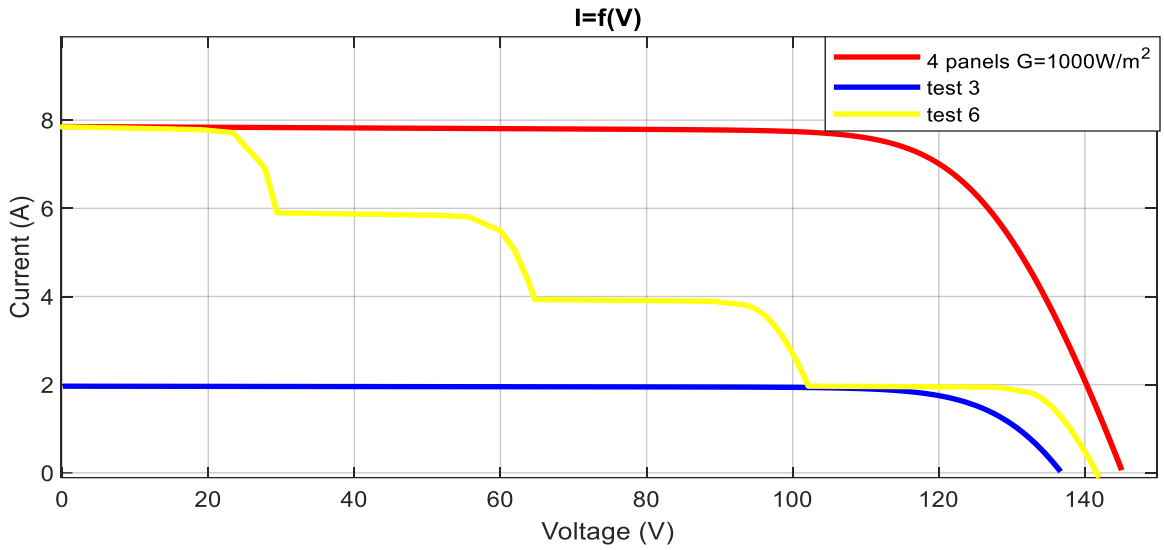

Figure II 21 Characteristic I-V of four parallel PV panels with partial shading (1000, 750,500, and 250 W/m2) with a diode and without diode

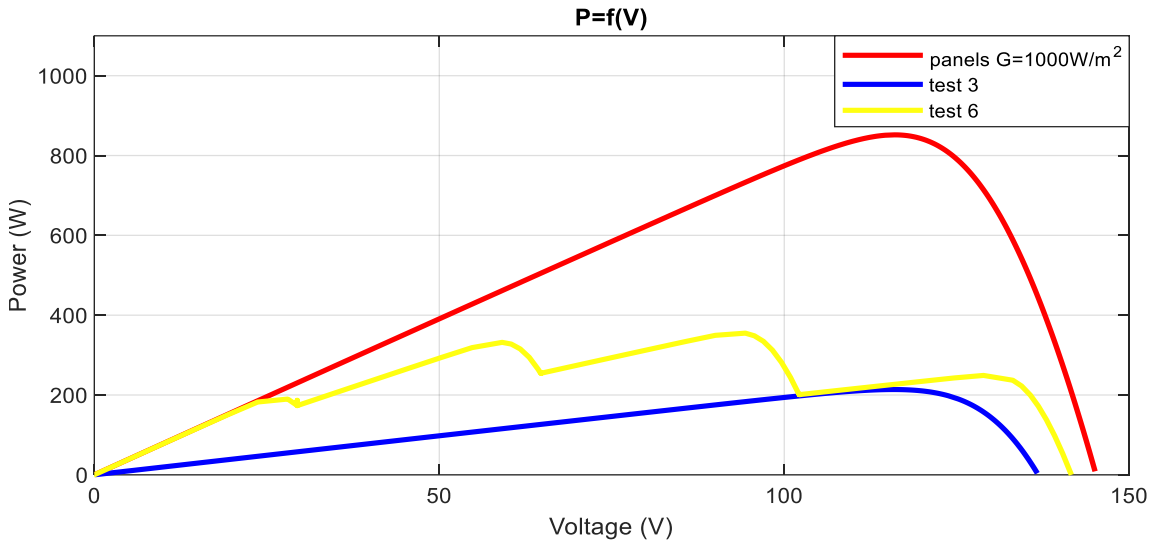

Figure II 22 Characteristic P-V of four parallel PV panels with partial shading (1000, 750,500, and 250 W/m2) with a diode and without diode

The results of the simulation lead us to the conclusion that shading a PV module has significant effects on its power-voltage curve (P V). Even if only a small portion of the module or the cell is shaded, the result is a significant decrease in the amount of power generated.

The Maximum Power Point (MPP), or the point at which a PV array is operating optimally, is different for each array. The intensity of the irradiation has the most impact on this power. The electrical characteristics of a solar generator's "String" are drastically altered if some of its modules are in the shadow. Power losses may be decreased and improved profitability can be ensured by utilizing bypass diodes, but because the photovoltaic generator now has several peaks on the I-V and P-V characteristics, it has distinct functioning points.

Another approach is being used by a number of researchers to enhance the performance of the PV generator; this approach entails switching the connections between the various cells or modules in order to discover a lucrative and effective configuration.

II.5 Modeling and presentation of the different PV configurations:

Connecting modules in diverse configurations can indeed be necessary and beneficial in various contexts. Different configurations can offer unique advantages and cater to specific requirements, in this part we used 5x5 PV modules to study four configurations (Series parallel (SP), Total Cross Tried (TCT), Bridge Link (BL), Honey-Comb (HC)) under partial shading.

II.5.1 Series parallel (SP):

Among all alternative PV array connections, SP is the most straightforward, reliable, and affordable option. Consequently, it is the setting that most programs utilize the most frequently.

the positive (+) terminal of one solar module is connected to the negative (-) terminal of another solar module, which increases the voltage(v) of the solar array. In parallel wiring, the positive (+) terminals and negative (-) terminals of each panel are connected together respectively, which increases the current(I) of the array.[38, 39]

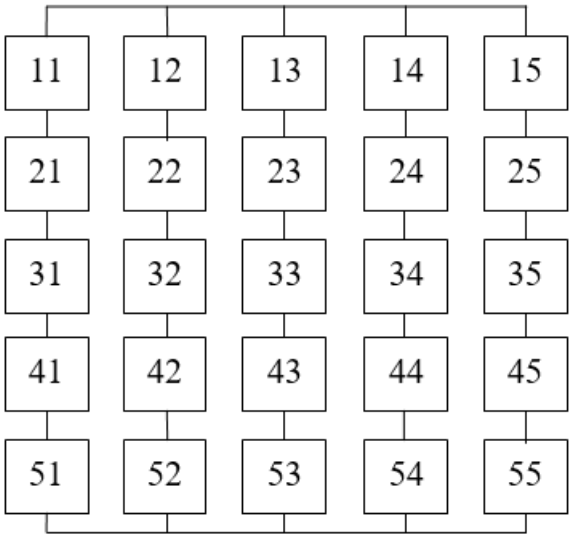

Figure II 23 SP configuration

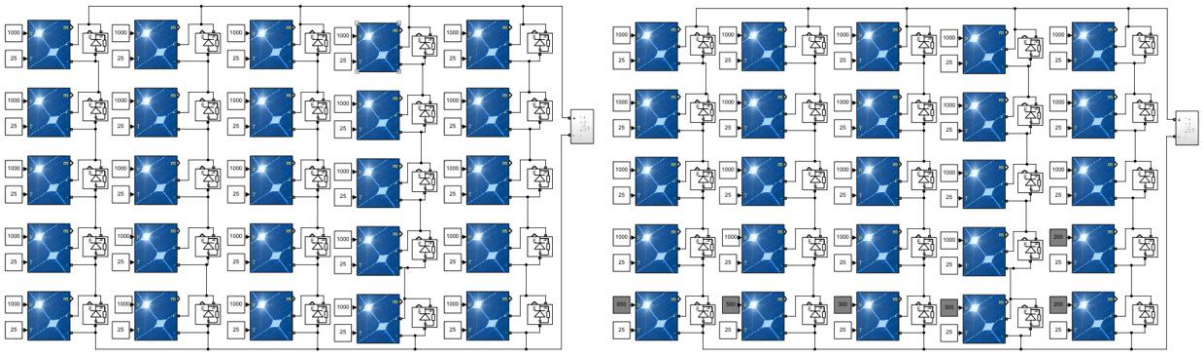

Figure II 24 Configuring SP in Simulink

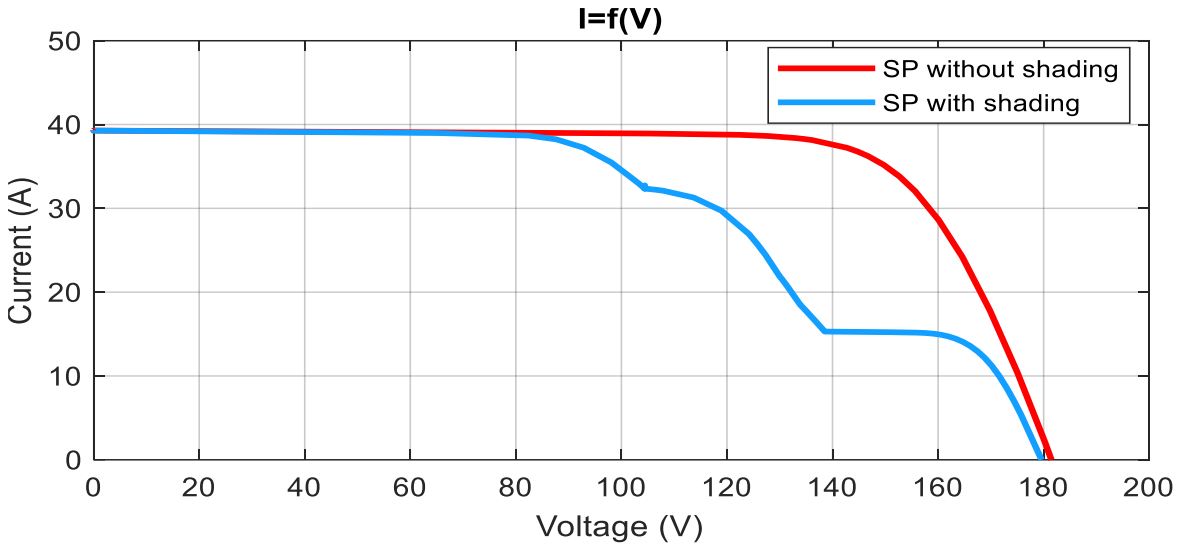

Figure II 25 I-V characteristic for SP under partial shading

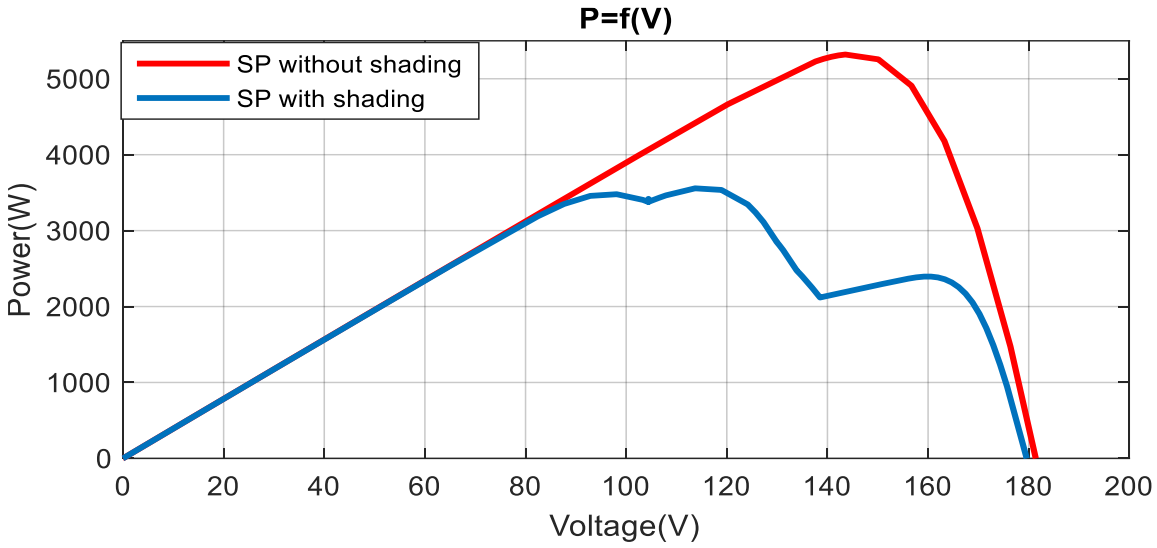

Figure II 26 P-V characteristic for SP Under partial shading

II.5.2 Total Cross Tried (TCT):

In TCT configuration is a photovoltaic (PV) array configuration that all the modules in one row have connected in parallel through a common link. to minimize the effect of shading on the power output of the PV system. In a TCT array, each solar cell is connected to its adjacent cells in both series and parallel, forming a grid-like structure.[38, 39]

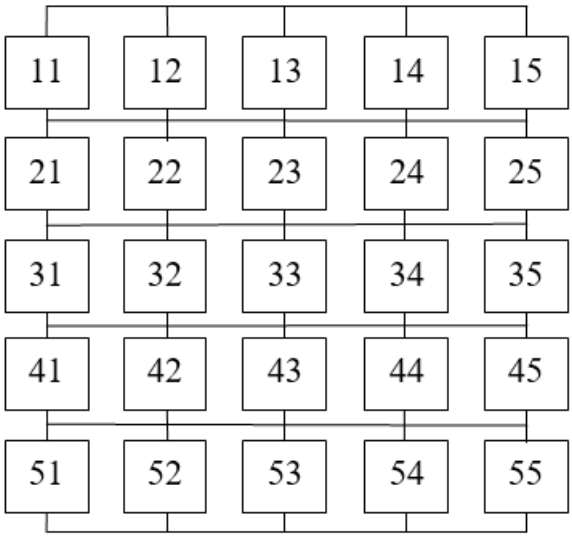

Figure II 27 TCT configuration

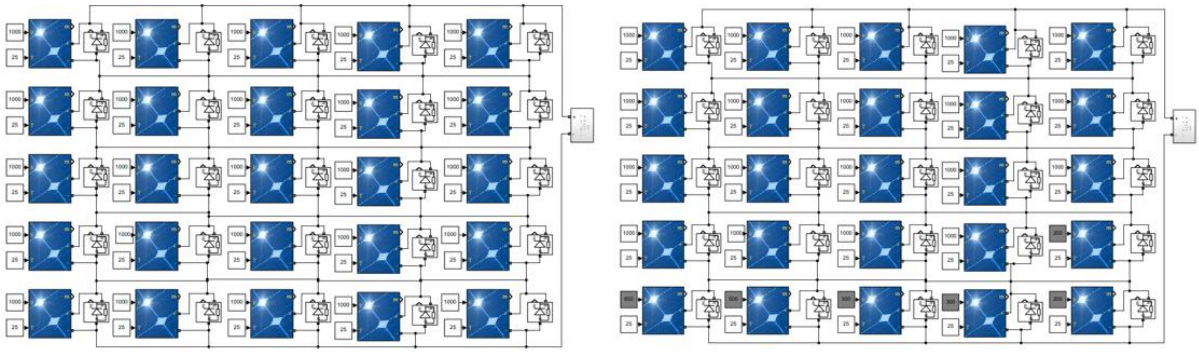

Figure II 28 Configuring TCT in Simulink

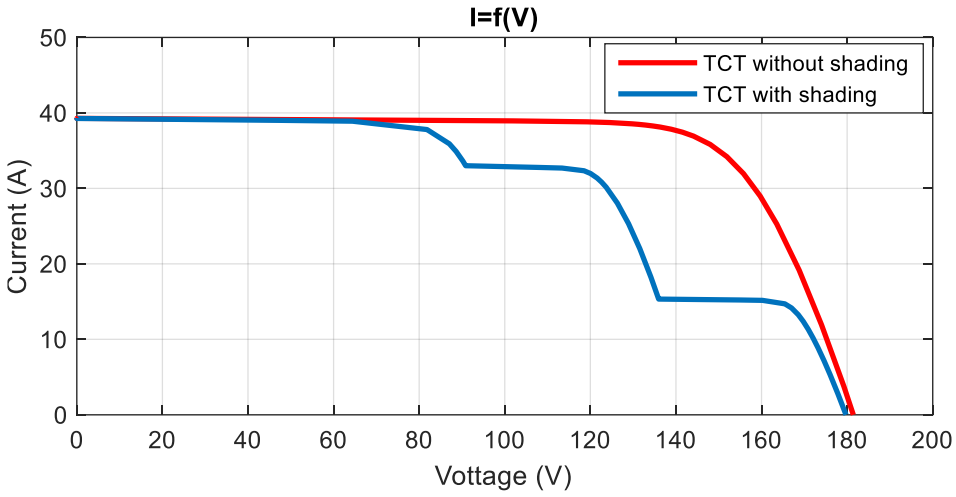

Figure II 29 I-V characteristic for TCT Under partial shading

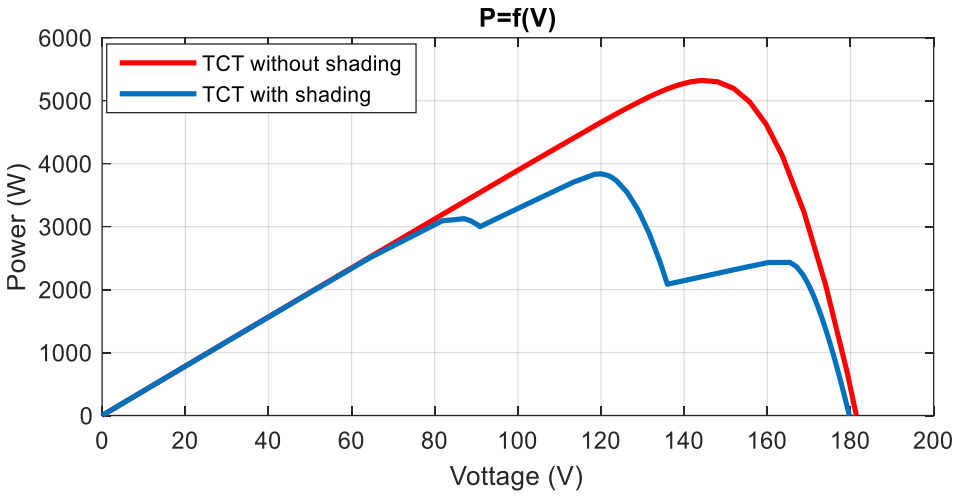

Figure II 30 P-V characteristic for TCT Under partial shading

II.5.3 Bridge Link (BL):

A Bridge-Linked (BL) PV array configuration reduces losses in Series-Parallel (SP) setup by connecting all of the modules in a bridge rectifier structure. two modules are series connected and then connected in parallel.[38, 39]

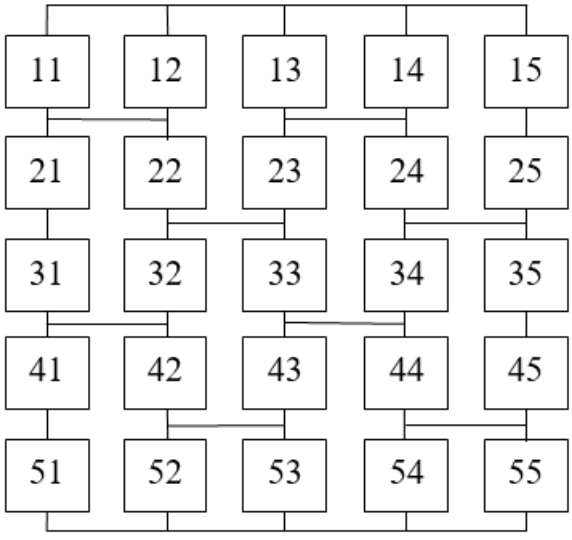

Figure II 31 BL configuration

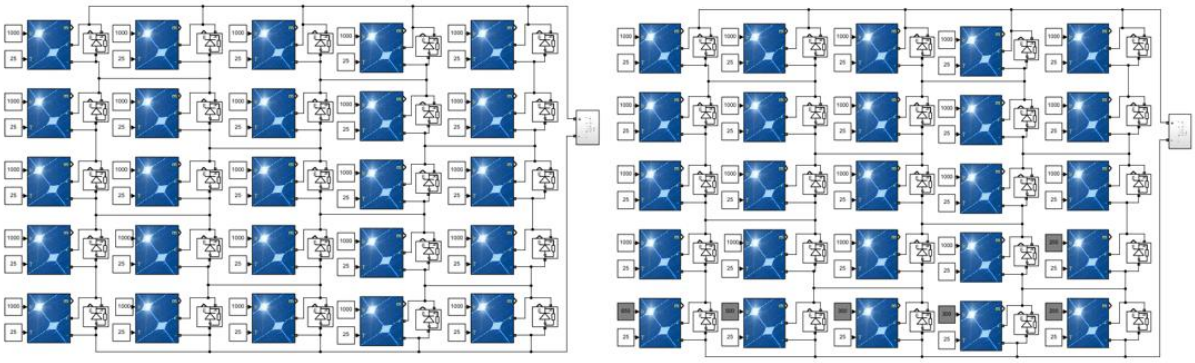

Figure II 32 Configuring BL in Simulink

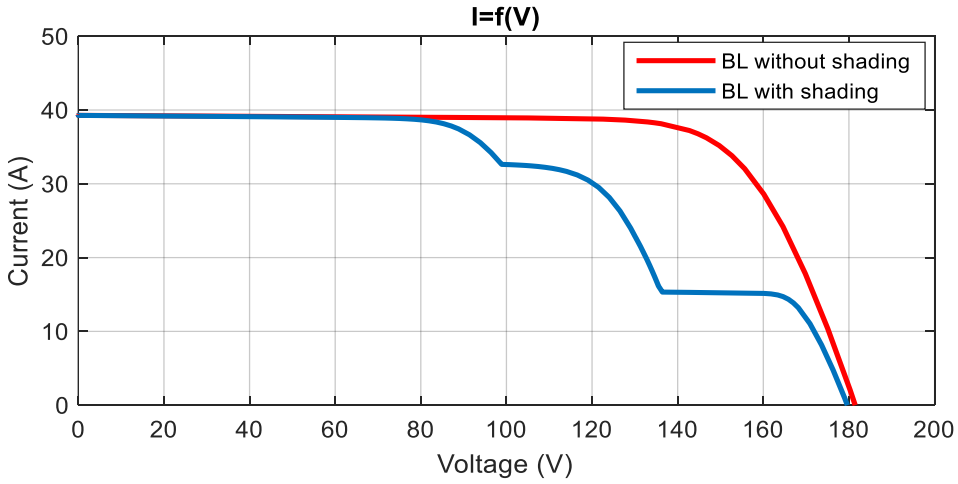

Figure II 33 I-V characteristic for BL Under partial shading

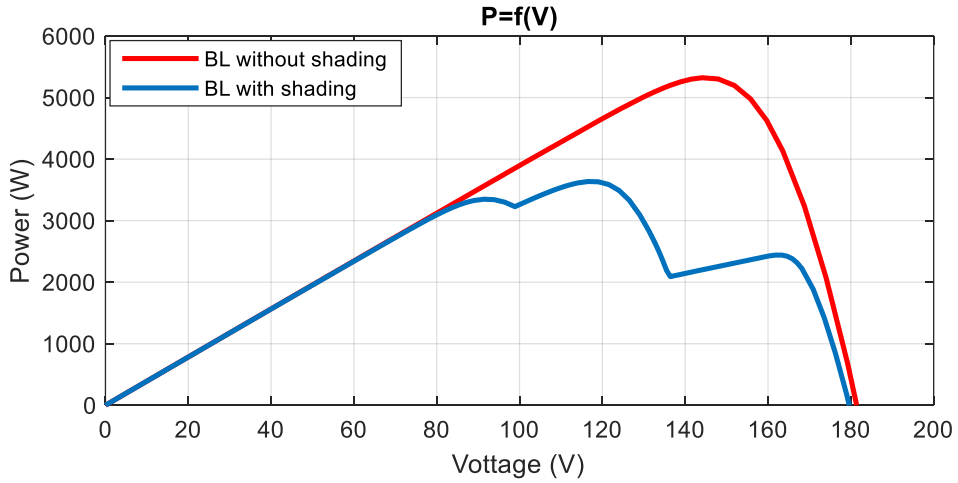

Figure II.31 P-V characteristic for BL under partial shading

II.5.4 Honey-Comb (HC):

A honeycomb (HC) PV array is a kind of solar panel system that makes use of solar panels in a honeycomb pattern that are hexagonal in form. The panels' ability to absorb solar irradiation from various angles and reflect it back onto nearby panels provides for optimal energy absorption and efficiency.[38, 39]

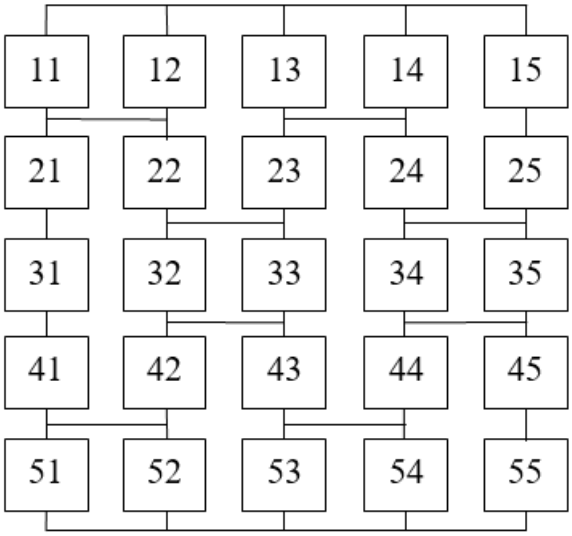

Figure II 34 HC configuration

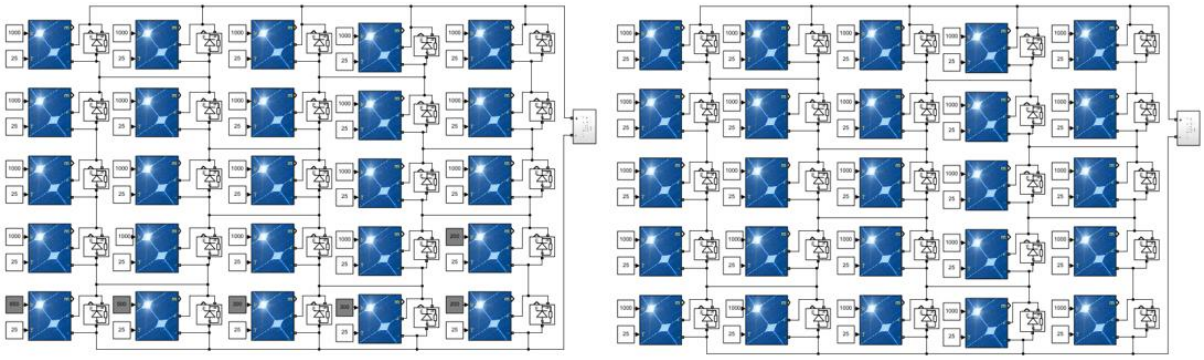

Figure II 35 Configuring HC in Simulink

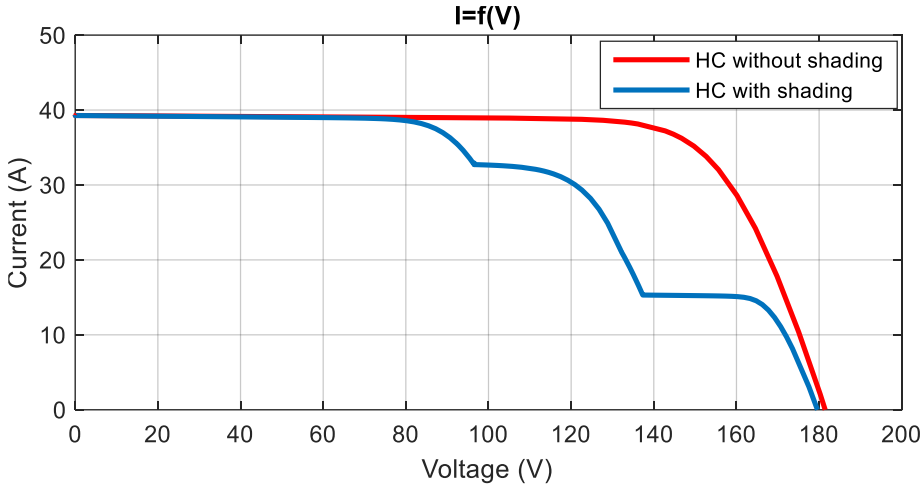

Figure II 36 I-V characteristic for HC under partial shading

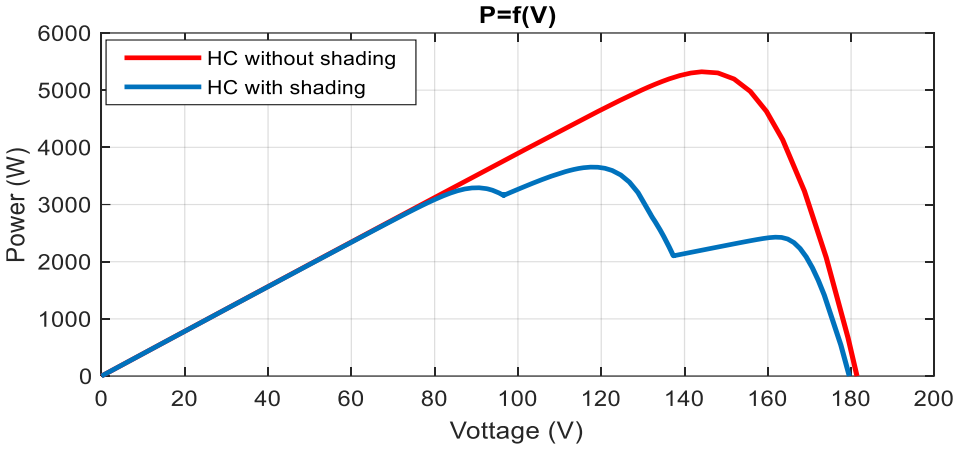

Figure II 37 P-V characteristic for HC under partial shading

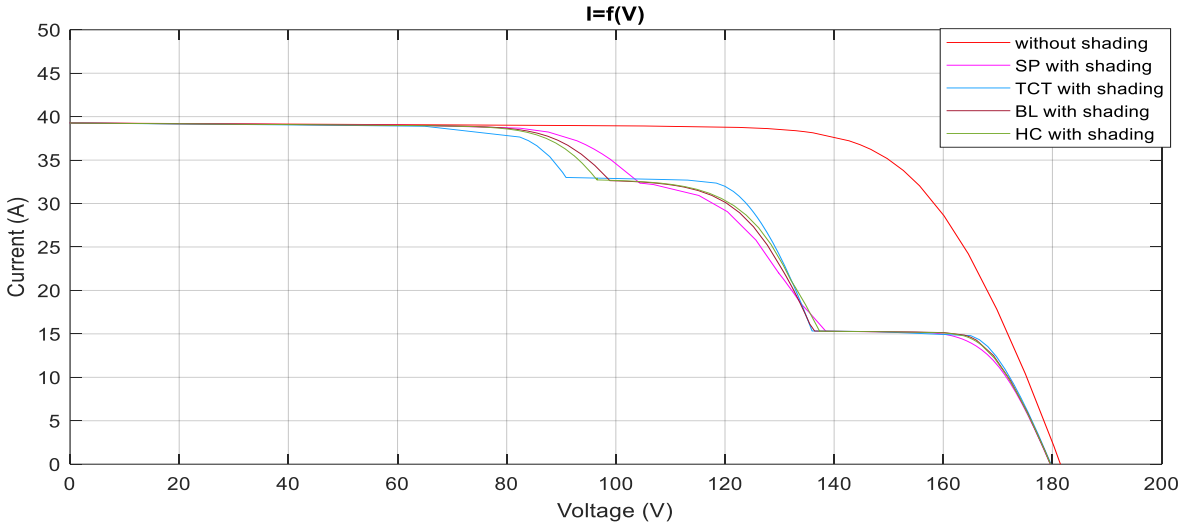

Figure II 38 I-V characteristics of different Configuring under partial shading

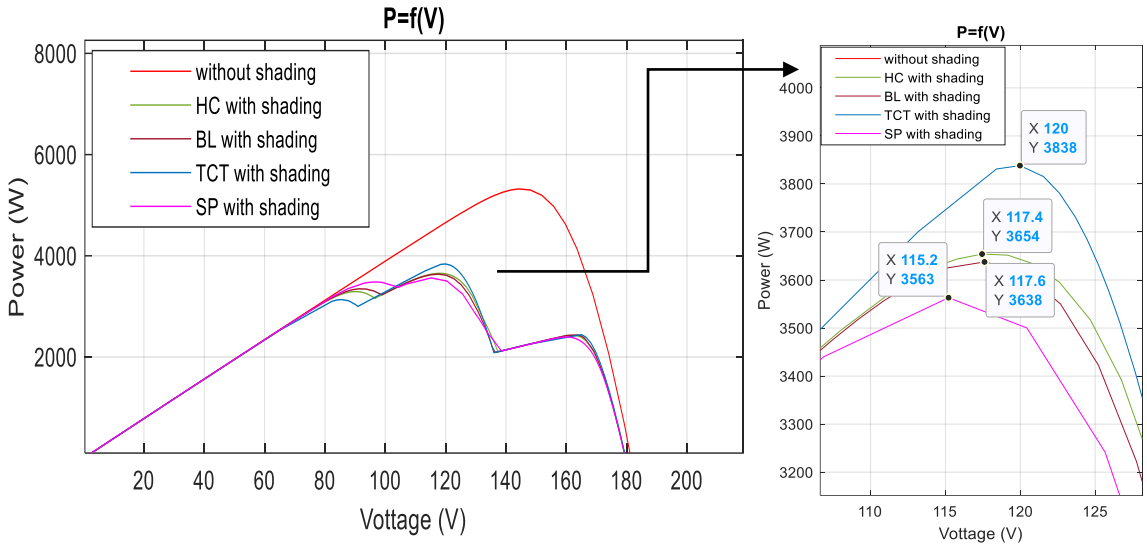

Figure II 39 P-V characteristics of different Configuring under partial shading

Measured values at each scenario configuration:

Table II-I Measured values at each scenario configuration

Configuration	PPM(W)	Voc (V)	Isc (A)	Vmp (V)	Imp (A)	FF%
SP	3536	179.58	39.26	115.2	30.69	50.14
TCT	3838	179.72	39.26	120	31.99	54.4
BL	3638	179.62	39.26	117.6	30.93	51.58
HC	3645	179.57	39.26	117.4	31.04	51.77

II.6 CONCLUSION:

In this chapter, we have studied a set of strategies for PV module configurations to improve energy efficiency in the PV field.

SP, BL, HC, TCT PV panel configurations performed in the presence of partial shading and analyzed using the single diode model under MATLAB/Simulink.

The results obtained showed that the performance of TCT configurations is the best configuration to improve the photovoltaic performance.

III) CHAPITRE III: Power optimization of a PV array in a partially shaded TCT configuration by using the Futoshiki technique

III.1 Introduction:

In this chapter, we are particularly to improve the bonding efficiency of Total Cross Tide (TCT) configurations in photovoltaic (PV) arrays by Futoshiki technique.

in the first part:

Using a 5x5 PV array with a TCT connection, the suggested technique of shade dispersal is demonstrated. Four different conventional shading conditions are used to analyze the array. MATLAB Simulink is used for simulation to locate the Global Maximum Power Point (GMPP) for the TCT and Futoshiki systems. The 5x5 PV array's power-voltage and mismatch loss (ML)-shading factor (SF) characteristics are graphed for both TCT and Futoshiki designs under all four types of shading.

In the second part:

For better results we considered a 9×9 PV array for TCT connection under different shader scenarios, which was simulated using MATLAB simulation, and optimized by Futoshiki technique. in different shader scenarios.

III.2 Different types of shading conditions:

Variations in shade coverage impacted can be seen when discussing partial shading circumstances. Here are different types of partial shading conditions based on shading coverage

III.2.1 Short and wide Shading:

This type of shading condition refers to situations where the shaded area covers a relatively large portion of the solar panel or array It can occur due to factors like clouds large objects or wide obstructions that cast shadows over a significant portion of the panel surface[40, 41]

III.2.2 Long and wide Shading:

Long and wide shading conditions involve shading that covers a substantial portion of the solar panel or array It can be caused by factors like large obstructions structures or vegetation that cast wide and elongated shadows across the panel surface. **[40, 41]**

III.2.1 Short and narrow:

Short and narrow shading conditions occur when shading covers a smaller more localized area of the solar panel or array It can be caused by narrow objects adjacent

structures or obstructions that create narrow concentrated shadows on the panel surface. [40, 41]

III.2.2 Long and narrow:

Long and narrow shading conditions involve shading that affects a narrow strip or portion of the solar panel or array. It can be caused by factors like nearby structures, objects, or obstructions that cast elongated, narrow shadows on the panel surface.[40, 41]

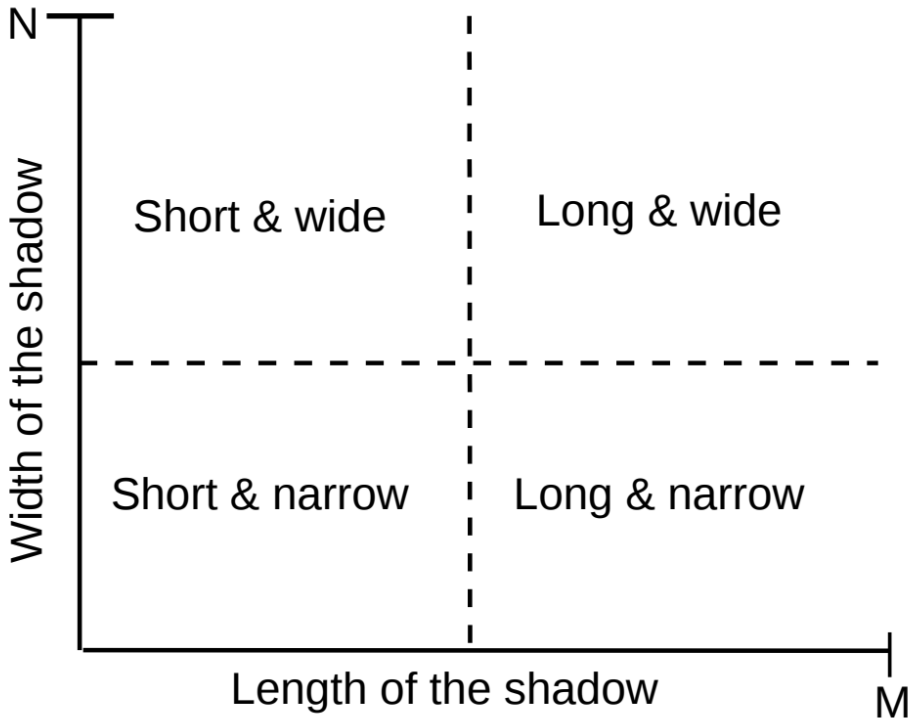

Figure III 1 The four distinct sorts of shadows[40]

These different types of partial shading conditions have varying effects on the performance of solar panels They can result in power losses mismatch issues or localized temperature variations.

III.3 Futoshiki puzzle:

The Futoshiki puzzle is indeed a challenging numeric puzzle that originated in Japan and has gained popularity worldwide. It is often categorized as a logic puzzle and is known for its unique rules and grid-based format. The puzzle is given as an n x n grid of cells and your goal is to complete the grid by filling in the remaining empty squares following specific

rules. Though the puzzle is very similar to "Sudoku" there is a difference such that it contains inequality signs between some adjacent cells

The main rules of Futoshiki puzzles are as follows:

Each row and column must contain unique numbers from 1 to the size of the grid (e.g., 1 to 5 for a 5x5 grid).

Some squares may have inequality signs ("<" or ">") indicating the relative values between adjacent squares. These signs must be respected when filling in the numbers.[42, 43]

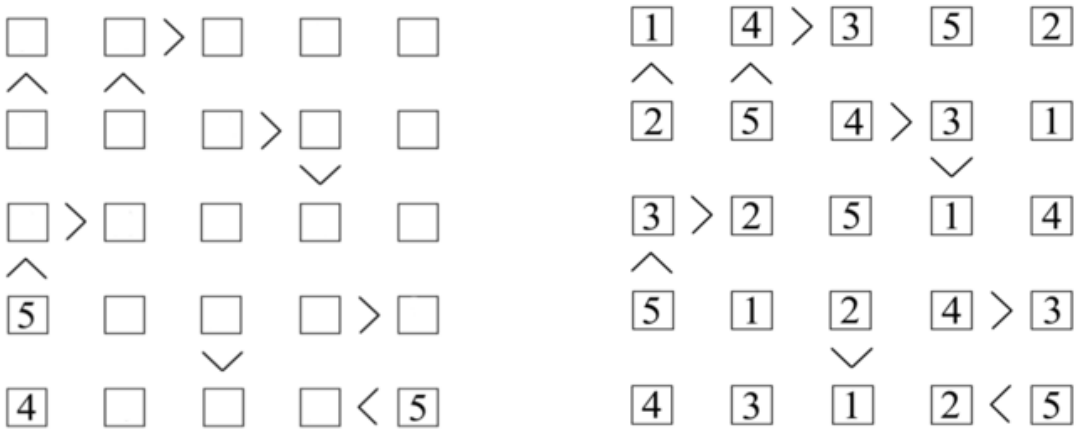

Figure III 2 Illustrative Example of Futoshiki Puzzle (5x5 grid)[44]

III.4 Futoshiki Configuration of a PV Array:

The reference to the Futoshiki puzzle technique in the context of array reconfiguration is not a conventional practice in the field of photovoltaic. and their application in array reconfiguration is metaphorical rather than a specific technique. The mention of the Futoshiki puzzle technique may imply a creative and logical approach to solving array reconfiguration problems where the goal is to find an optimal arrangement or configuration that minimizes losses and maximizes power output. [44]

(A). TCT (B). futoshiki

11	12	13	14	15
21	22	23	24	25
31	32	33	34	35
41	42	43	44	45
51	52	53	54	55

11	42	33	54	25
21	52	43	34	15
31	22	53	14	45
51	12	23	44	35
41	32	13	24	55

Figure III 3 A 5x5 PV ARRAY IN DIFFERENT CONFIGURATION[44]

Theoretical and Simulation Results for Power Enhancement:

In order to illustrate each scenario, we have defined our photovoltaic system as a finite-dimensional matrix Ln × p, where n ∈ IN* denotes the number of modules per rows and p ∈ IN* represents the number of modules per columns. The n rows are horizontal and the p columns are vertical. Each element a C, R (C= 1 to 5 and R= 1 to 5) of a matrix represents a module. For example, 5,2 represents the modulus in the Fifth row and secondly column of the matrix L. The module is placed as follows:

$$L_{C\times R} = \begin{bmatrix} a_{11} & a_{12} & a_{13} & a_{14} & a_{15} \\ a_{21} & a_{22} & a_{23} & a_{24} & a_{25} \\ a_{31} & a_{31} & a_{33} & a_{34} & a_{35} \\ a_{41} & a_{42} & a_{43} & a_{44} & a_{45} \\ a_{51} & a_{52} & a_{53} & a_{54} & a_{55} \end{bmatrix}$$

III.5 The first part:

III.5.1 Short and wide Shading Condition (SW):

The modules of a PV array get three distinct types of solar irradiation under SW shadowing conditions, as indicated in (The matrix), including 940 W/m2, 550 W/m2, and 200 W/m2. To locate the GMPP, A PV array's current must be calculated for each row, according to the following relationship:

$$\mathbf{I} = \left(\frac{\mathbf{G}}{\mathbf{G_{STS}}}\right) \times \mathbf{I_m} \qquad \text{(III.1)}$$

where (Im) is the current produced by the module under standard test conditions, which include standard temperature (T=25°C) and standard irradiation GSTC (G= 1000 W/m^2). The voltage of the array is determined using the following equation and Kirchhoff's voltage law:

$$\boldsymbol{V} = \sum_{\mathbf{x=1}}^{\mathbf{5}} \mathbf{V_{mx}} \qquad \text{(III.2)}$$

where Vmx is the voltage of the xth row of a PV array.

It is assumed in the current computation that all of the PV array's modules are producing the same current Im under standard test conditions (STC). The current across rows 1 to 3 in the TCT setup is computed as follows since each module receives the same 940 W/m2 of irradiation:

The first three and following two modules in rows 4 and 5 of a PV array get solar irradiation of 550 W/m2 and 200 W/m2, respectively. Thus, the following formula is used to determine the current between rows 4 and 5:

$$\mathbf{IR4 = IR5 = 3 \times 0.55\,Im + 2 \times 0.2\,Im = 2.02\,Im} \quad \text{(III.3)}$$

The different irradiation values for this scenario are presented in the following matrix:

$$L_{5\times5} = \begin{bmatrix} 940 & 940 & 940 & 940 & 940 \\ 940 & 940 & 940 & 940 & 940 \\ 940 & 940 & 940 & 940 & 940 \\ 550 & 550 & 550 & 200 & 200 \\ 550 & 550 & 550 & 200 & 200 \end{bmatrix} {}^{W}/_{m^2}\ a\ T = 25°$$

(TCT)

$$L_{5\times5} = \begin{bmatrix} 940 & 550 & 550 & 940 & 940 \\ 940 & 940 & 550 & 200 & 940 \\ 940 & 550 & 940 & 940 & 200 \\ 550 & 940 & 940 & 200 & 940 \\ 550 & 940 & 940 & 940 & 200 \end{bmatrix} {}^{W}/_{m^2}\ a\ T = 25°$$

(Futoshiki)

The shading pattern of the Futoshiki configuration is known as "shade dispersion with Futoshiki configuration" and the current across each row of a PV array is calculated using the following equations:

$$\mathbf{IR1 = 3 \times 0.94Im + 2 \times 0.55Im = 3.92Im} \quad \text{(III.4)}$$

$$\mathbf{IR5 = IR4 = IR3 = IR2 = 3 \times 0.94Im + 0.55Im + 0.2Im = 3.57Im} \quad \text{(III.5)}$$

Table III-I GMPP, SW shading situation, in TCT and futoshiki setup

TCT configuration			Futoshiki configuration		
*IR	Array Voltage (V)	Array Power (P)	*IR	Array Voltage (V)	Array Power (P)
IR1 4.7 Im	Vm	4.7VmIm	IR1 3.92 Im	Vm	3.92VmIm
IR2 4.7 Im	2Vm	9.4VmIm	IR2 3.57 Im	2Vm	7.14VmIm
IR3 4.7 Im	3Vm	14.1VmIm	IR3 3.57 Im	3Vm	10.71VmIm
IR4 2.02 Im	4Vm	8.08VmIm	IR4 3.57 Im	4Vm	14.28VmIm
IR5 2.02 Im	5Vm	10.1VmIm	IR5 3.57 Im	5Vm	17.85VmIm

IR: the row current of a PV array

Vm: the voltage of each module at STC

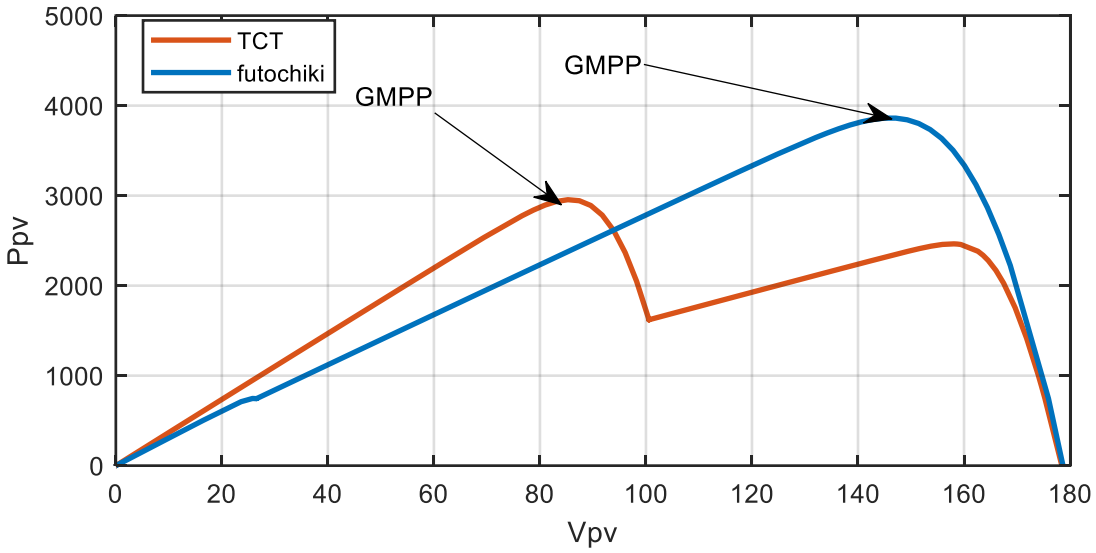

Figure III 4 P-V characteristics of different Configuring under partial shading (SW)

The voltages and row currents of a photovoltaic (PV) array in TCT and Futoshiki designs are shown in Table III I. The rows of the PV array with lower solar irradiation, denoted by low current, are bypassed in ascending order of module current in order to find the Global Maximum Power Point (GMPP). The PV array's voltage, disregarding minute voltage changes in each row, is 5Vm if any row is not bypassed. Bypassing the PV modules in the second row reduces the array's voltage to 3Vm while maintaining the diode voltage. According to Table III I, the voltage of the array is determined depending on the quantity of bypassed rows.

It is shown that, in the TCT design of a PV array, when rows 5 and 4 are bypassed, the GMPP occurs at a decreased voltage level, greatly deviating from the Maximum Power Point (MPP) voltage. On the other hand, with the suggested arrangement (Futoshiki), the GMPP lines up with the array's MPP voltage. In the TCT and Futoshiki setups, the power produced at the GMPP is 14.1VmIm and 17.85VmIm, respectively. As a result, the potential power increase in the suggested architecture over the TCT configuration is 26.59%.

A power-voltage simulation of the PV array is run using MATLAB to test the theoretical conclusions. The results are shown in Figure III 4. According to the simulation, the highest power generated by the Futoshiki and TCT layouts is 2955W and 3863W, respectively. As a result, the maximum power generated by the Futoshiki design is 30.72% greater than that of the TCT arrangement. Notably, the suggested design shifts the GMPP, which occurs at a low voltage in the TCT structure, to the MPP voltage of the PV array. Due

to the scattered shading effects across the array, the power generated in the suggested design exceeds that of the TCT.

III.5.2 Long and wide Shading Condition (LW):

PV array modules receive four distinct types of solar irradiation under LW shading conditions, as shown in (matrix), including 940 W/m2,720 W/m2, 550 W/m2, and 200 W/m2, the different irradiation values for this scenario are presented in the following matrix:

$$L_{5\times5} = \begin{bmatrix} 940 & 940 & 940 & 720 & 720 \\ 940 & 940 & 940 & 720 & 720 \\ 940 & 940 & 940 & 720 & 720 \\ 550 & 550 & 550 & 200 & 200 \\ 550 & 550 & 550 & 200 & 200 \end{bmatrix} {}^{w}/_{m^2} \; a\; T = 25°$$

(TCT)

$$L_{5\times5} = \begin{bmatrix} 940 & 550 & 550 & 720 & 720 \\ 940 & 940 & 550 & 200 & 720 \\ 940 & 550 & 940 & 720 & 200 \\ 550 & 940 & 940 & 200 & 720 \\ 550 & 940 & 940 & 720 & 200 \end{bmatrix} {}^{w}/_{m^2} \; a\; T = 25°$$

(Futoshiki)

the following equations may be used to determine the current flowing through each row of a PV array.

For TCT:

$$\mathbf{IR1 = IR2 = IR3 = 3 \times 0.94Im + 2 \times 0.72Im = 4.26m} \quad \text{(III.6)}$$

$$\mathbf{IR4 = IR5 = 3 \times 0.55\ Im + 2 \times 0.2\ Im = 2.02\ Im} \quad \text{(III.7)}$$

For futoshiki:

$$\mathbf{IR1 = 0.94Im + 2 \times 0.72Im + 2 \times 0.55Im = 3.48Im} \quad \text{(III.8)}$$

$$\mathbf{IR5 = IR4 = IR3 = IR2 = 2 \times 0.94Im + 0.72Im + 0.55Im + 0.2Im = 3.35Im} \quad \text{(III.9)}$$

Table III-II GMPP, LW shading situation, in TCT and futoshiki setup

TCT configuration			Futoshiki configuration		
*IR	Array Voltage (V)	Array Power (P)	*IR	Array Voltage (V)	Array Power (P)
IR1 4.26 Im	Vm	4.26VmIm	IR1 3.48 Im	Vm	3.48VmIm
IR2 4.26 Im	2Vm	8.52VmIm	IR2 3.35 Im	2Vm	6.7VmIm
IR3 4.26 Im	3Vm	12.78VmIm	IR3 3.35 Im	3Vm	10.05VmIm
IR4 2.02 Im	4Vm	8.08VmIm	IR4 3.35 Im	4Vm	13.4VmIm
IR5 2.02 Im	5Vm	10.1VmIm	IR5 3.35 Im	5Vm	16.75VmIm

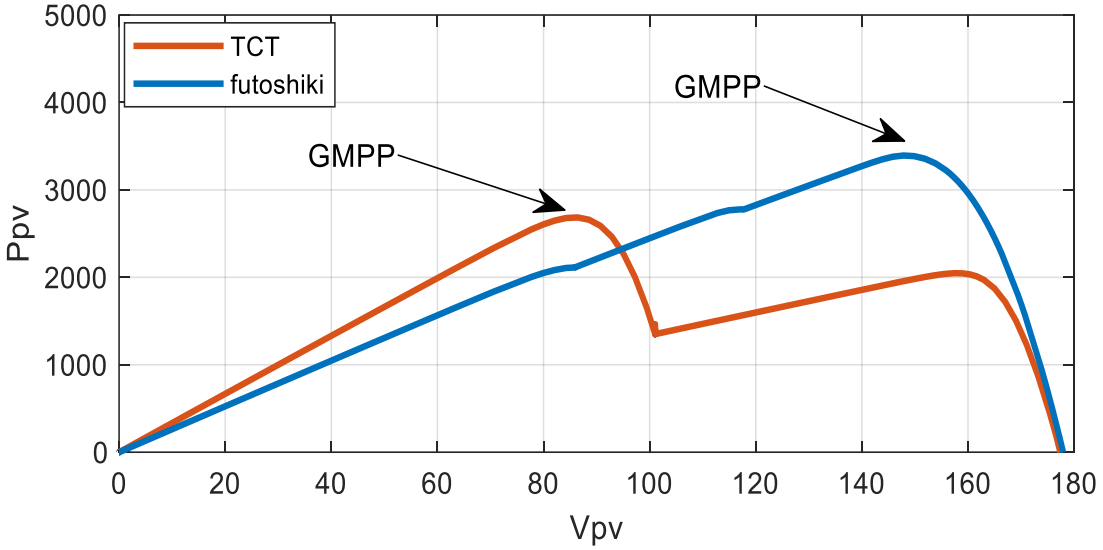

Figure III 5 P-V characteristics of different Configuring under partial shading (LW)

Table III II provides information on a PV array's power, voltage, and current distribution across each row. The power generated at GMPP in the TCT and Futoshiki configurations is 12.78 VmIm and 16.75 VmIm, respectively, as can be observed from Table III II. As a result, the theoretically predicted power improvement for the suggested design relative to TCT is 31.06%. According to Figure III 5, the maximum power produced by the TCT and the suggested design are 2685 W and 3393 W, respectively. Therefore, the suggested arrangement's maximum power output is 26.36% larger than the TCT configuration.

III.5.3 Short and narrow Shading Condition (SN):

PV array modules receive three distinct types of solar irradiation under SN shading conditions, as shown in (matrix), including 940 W/m2, 550 W/m2, and 470 W/m2, the different irradiation values for this scenario are presented in the following matrix:

$$L_{5\times5} = \begin{bmatrix} 940 & 940 & 940 & 940 & 940 \\ 940 & 940 & 940 & 940 & 940 \\ 940 & 940 & 940 & 940 & 940 \\ 940 & 940 & 940 & 470 & 470 \\ 940 & 940 & 940 & 550 & 550 \end{bmatrix} {}^{w}/_{m^2} \; a\; T = 25°$$

(TCT)

$$L_{5\times5} = \begin{bmatrix} 940 & 940 & 940 & 940 & 940 \\ 940 & 940 & 940 & 550 & 940 \\ 940 & 940 & 940 & 940 & 470 \\ 940 & 940 & 940 & 470 & 940 \\ 940 & 940 & 940 & 940 & 550 \end{bmatrix} {}^{w}/_{m^2} \; a\; T = 25°$$

(Futoshiki)

the following equations may be used to determine the current flowing through each row of a PV array.

For TCT:

$$\mathbf{IR1 = IR2 = IR3 = 5 \times 0.94Im = 4.7Im} \quad \text{(III.10)}$$

$$\mathbf{IR4 = 3 \times 0.94Im + 2 \times 0.47Im = 3.74Im} \quad \text{(III.11)}$$

$$\mathbf{IR5 = 3 \times 0.94Im + 2 \times 0.55Im = 3.92Im} \quad \text{(III.12)}$$

For futoshiki:

$$\mathbf{IR1 = 5 \times 0.94Im = 4.7Im} \quad \text{(III.13)}$$

$$\mathbf{IR2 = IR5 = 4 \times 0.94Im + 0.55Im = 4.31Im} \quad \text{(III.14)}$$

$$\mathbf{IR3 = IR4 = 4 \times 0.94Im + 0.47Im = 4.23Im} \quad \text{(III.15)}$$

Table III-III GMPP, SN shading situation, in TCT and futoshiki setup

TCT configuration			Futoshiki configuration		
*IR	Array Voltage (V)	Array Power (P)	*IR	Array Voltage (V)	Array Power (P)
IR1 4.7 Im	Vm	4.7VmIm	IR1 4.7 Im	Vm	4.7VmIm
IR2 4.7 Im	2Vm	9.4VmIm	IR2 4.31 Im	2Vm	8.62VmIm
IR3 4.7 Im	3Vm	14.1VmIm	IR3 4.23 Im	3Vm	12.62VmIm
IR4 3.74 Im	4Vm	14.96VmIm	IR4 4.23 Im	4Vm	16.62VmIm
IR5 3.92 Im	5Vm	19.6VmIm	IR5 4.31 Im	5Vm	21.55VmIm

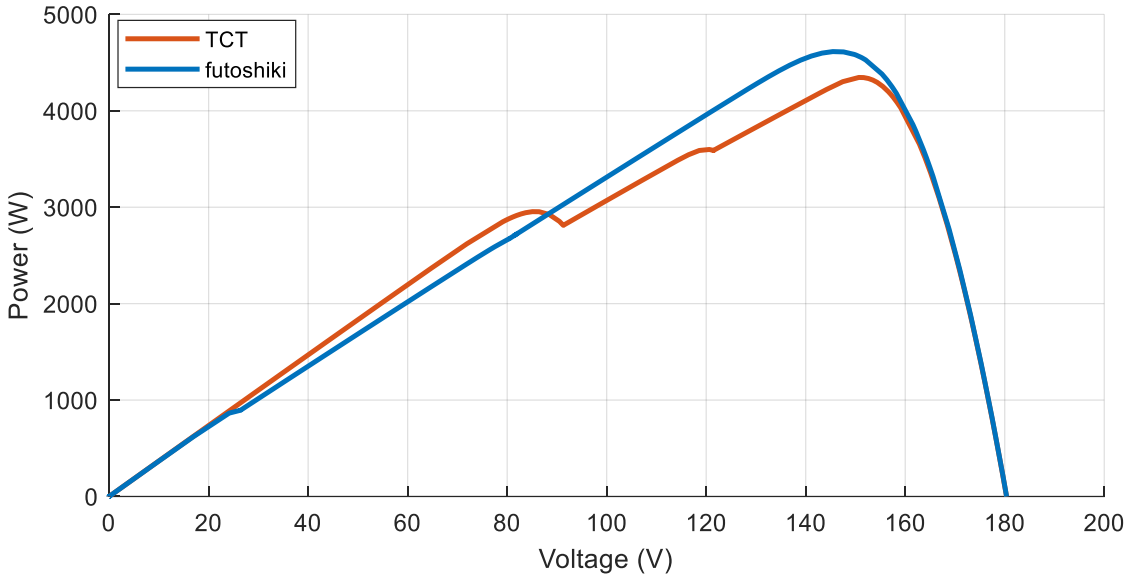

Figure III 6 P-V characteristics of different Configuring under partial shading (SN)

The suggested configuration and theoretically computed location of the GMPP are displayed in Table III-III. In the TCT and suggested configurations, the power produced at GMPP is 19.6VmIm and 21.55VmIm, respectively. Therefore, the theoretically predicted power improvement for the suggested arrangement relative to the TCT configuration is 9.94%.

The highest power produced by the TCT and Futoshiki configurations, respectively, are 4346 W and 4614 W, as shown in Figure III 6. Consequently, the maximum power produced by the suggested arrangement is 6.16% greater than that of the TCT setup.

III.5.4 Long and narrow Shading Condition (LN):

PV array modules receive three distinct types of solar irradiation under SN shading conditions, as shown in (matrix), including 940 W/m2, 600 W/m2, and 470 W/m2, the different irradiation values for this scenario are presented in the following matrix:

$$L_{5\times5} = \begin{bmatrix} 940 & 940 & 940 & 940 & 940 \\ 940 & 940 & 940 & 600 & 600 \\ 940 & 940 & 940 & 600 & 600 \\ 940 & 940 & 940 & 470 & 470 \\ 940 & 940 & 940 & 470 & 470 \end{bmatrix} {}^{w}/_{m^2}\ a\ T = 25°$$

(TCT)

$$L_{5\times5} = \begin{bmatrix} 940 & 940 & 940 & 600 & 600 \\ 940 & 940 & 940 & 470 & 940 \\ 940 & 940 & 940 & 600 & 470 \\ 940 & 940 & 940 & 470 & 600 \\ 940 & 940 & 940 & 940 & 470 \end{bmatrix} {}^{w}/_{m^2}\ a\ T = 25°$$

(Futoshiki)

the following equations may be used to determine the current flowing through each row of a PV array.

For TCT:

$$\mathbf{IR1 = 5\ \times 0.94Im = 4.7Im} \quad \text{(III.16)}$$

$$\mathbf{IR2 = IR3 = 3 \times 0.94Im + 2\ \times 0.6Im = 4.02Im} \quad \text{(III.17)}$$

$$\mathbf{IR4 = IR5 = 3\ \times 0.94Im + 2\ \times 0.47Im = 3.76Im} \quad \text{(III.18)}$$

For futoshiki:

$$\mathbf{IR1 = 3\ \times 0.94Im + 2\ \times 0.6Im = 4.01Im} \quad \text{(III.19)}$$

$$\mathbf{IR2 = IR5 = 4\ \times 0.94Im + 0.47Im = 4.23Im} \quad \text{(III.20)}$$

$$\mathbf{IR3 = IR4 = 3\ \times 0.94Im + 0.6Im + 0.47Im = 3.89Im} \quad \text{(III.21)}$$

Table III-IV GMPP, LN shading situation, in TCT and futoshiki setup

TCT configuration			Futoshiki configuration		
*IR	Array Voltage (V)	Array Power (P)	*IR	Array Voltage (V)	Array Power (P)
IR1 4.7 Im	Vm	4.7VmIm	IR1 4.01 Im	Vm	4.01VmIm
IR2 4.02 Im	2Vm	8.04VmIm	IR2 4.23 Im	2Vm	8.46VmIm
IR3 4.02 Im	3Vm	12.06VmIm	IR3 3.89 Im	3Vm	11.67VmIm
IR4 3.76 Im	4Vm	15.04VmIm	IR4 3.89 Im	4Vm	15.56VmIm
IR5 3.76 Im	5Vm	18.8VmIm	IR5 4.23 Im	5Vm	21.15VmIm

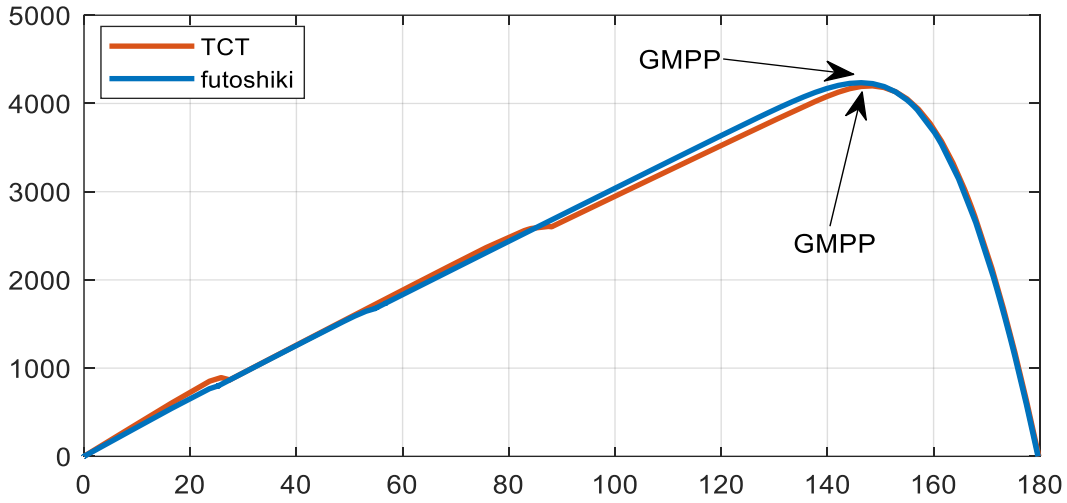

Figure III 7 P-V characteristics of different Configuring under partial shading (LN)

Table III-IV and Table IV display the TCT, Futoshiki, and shadow dispersion with Futoshiki configuration shading patterns. The Table III-IV displays the planned configuration and position of the GMPP of the TCT. In the TCT and suggested configurations, the power produced at GMPP is 18.8VmIm and 21.15VmIm, respectively. Therefore, the theoretically computed power improvement for the suggested arrangement relative to the TCT configuration is 12.5%.

The highest power produced by the TCT and Futoshiki configurations, respectively, is 4198 W and 4289 W, as can be shown in Figure III 7. Consequently, the maximum power generated by the Futoshiki arrangement is 2.16% greater than that of the TCT configuration. Although the power-voltage curve in a Futoshiki arrangement may have several peaks, they are not evident in the current study since the distribution of shadow across each row of the PV array is virtually equal.

III.6 the second part:

III.6.1 (9*9) Short and wide Shading Condition (SW):

As shown in (The matrix), a PV array's modules receive three different forms of solar irradiation: 940 W/m2, 550 W/m2, and 200 W/m2. A PV array's current must be determined for each row in order to determine where the GMPP is located.

$$L_{9\times9} = \begin{bmatrix} 940 & 940 & 940 & 940 & 940 & 940 & 940 & 940 & 940 \\ 940 & 940 & 940 & 940 & 940 & 940 & 940 & 940 & 940 \\ 940 & 940 & 940 & 940 & 940 & 940 & 940 & 940 & 940 \\ 940 & 940 & 940 & 940 & 940 & 940 & 940 & 940 & 940 \\ 940 & 940 & 940 & 940 & 940 & 940 & 940 & 940 & 940 \\ 550 & 550 & 550 & 550 & 550 & 200 & 200 & 200 & 200 \\ 550 & 550 & 550 & 550 & 550 & 200 & 200 & 200 & 200 \\ 550 & 550 & 550 & 550 & 550 & 200 & 200 & 200 & 200 \\ 550 & 550 & 550 & 550 & 550 & 200 & 200 & 200 & 200 \end{bmatrix} {}^{w}/_{m^2}\ a\ T = 25°$$

(TCT 9*9)

$$L_{9\times9} = \begin{bmatrix} 550 & 940 & 550 & 940 & 940 & 940 & 200 & 940 & 200 \\ 940 & 550 & 940 & 550 & 940 & 940 & 200 & 200 & 940 \\ 940 & 550 & 940 & 550 & 550 & 200 & 940 & 940 & 940 \\ 940 & 940 & 940 & 940 & 550 & 940 & 200 & 200 & 200 \\ 940 & 550 & 940 & 550 & 940 & 200 & 940 & 200 & 940 \\ 940 & 940 & 550 & 940 & 550 & 940 & 200 & 200 & 940 \\ 550 & 940 & 550 & 940 & 940 & 200 & 940 & 940 & 200 \\ 550 & 940 & 550 & 550 & 550 & 940 & 940 & 940 & 940 \\ 550 & 550 & 940 & 940 & 940 & 200 & 940 & 940 & 200 \end{bmatrix} {}^{w}/_{m^2}\ a\ T = 25°$$

(Futoshiki 9*9)[45]

the following equations may be used to determine the current flowing through each row of a PV array.

For TCT:

$$\mathbf{IR1 = IR2 = IR3 = IR4 = IR5 = 9\ \times 0.94Im = 8.46Im} \quad \text{(III.22)}$$

$$\mathbf{IR6 = IR7 = IR8 = IR9 = 5\ \times 0.55Im + 5\ \times 0.2Im = 3.55Im} \quad \text{(III.23)}$$

For futoshiki:

$$\mathbf{IR1 = IR2 = IR5 = IR6 = IR7 = IR9} \quad \text{(III.24)}$$

$$\mathbf{IR1 = 5\ \times 0.94Im + 2\ \times 0.2Im + \ 2 \times 0.55Im = 6.2Im} \quad \text{(III.25)}$$

$$\mathbf{IR3 = 5\ \times 0.94Im + 0.2Im + \ 3 \times 0.55Im = 6.55Im} \quad \text{(III.26)}$$

$$\mathbf{IR4 = 5\ \times 0.94Im + 3 \times 0.2Im + \ 0.55Im = 5.85Im} \quad \text{(III.27)}$$

$$\mathbf{IR8 = 5\ \times 0.94Im + 4 \times 0.55Im = 6.9Im} \quad \text{(III.28)}$$

Table III-V GMPP, SW shading situation, in TCT and futoshiki setup (9*9)

Short and wide Shading Condition (SW)					
TCT configuration			Futoshiki configuration		
*IR	Array Voltage (V)	Array Power (P)	*IR	Array Voltage (V)	Array Power (P)
IR1 8.46 Im	Vm	08.46 VmIm	IR1 6.20 Im	Vm	06.20 VmIm
IR2 8.46 Im	2Vm	16.92 VmIm	IR2 6.20 Im	2Vm	12.40 VmIm
IR3 8.46 Im	3Vm	25.38 VmIm	IR3 6.55 Im	3Vm	19.65 VmIm
IR4 8.46 Im	4Vm	33.84 VmIm	IR4 5.85 Im	4Vm	23.40 VmIm
IR5 8.46 Im	5Vm	42.30 VmIm	IR5 6.20 Im	5Vm	31.00 VmIm
IR6 3.55 Im	6Vm	21.30 VmIm	IR6 6.20 Im	6Vm	37.20 VmIm
IR7 3.55 Im	7Vm	24.85 VmIm	IR7 6.20 Im	7Vm	43.40 VmIm
IR8 3.55 Im	8Vm	28.40 VmIm	IR8 6.90 Im	8Vm	55.20 VmIm
IR9 3.55 Im	9Vm	31.95 VmIm	IR9 6.20 Im	9Vm	55.80 VmIm

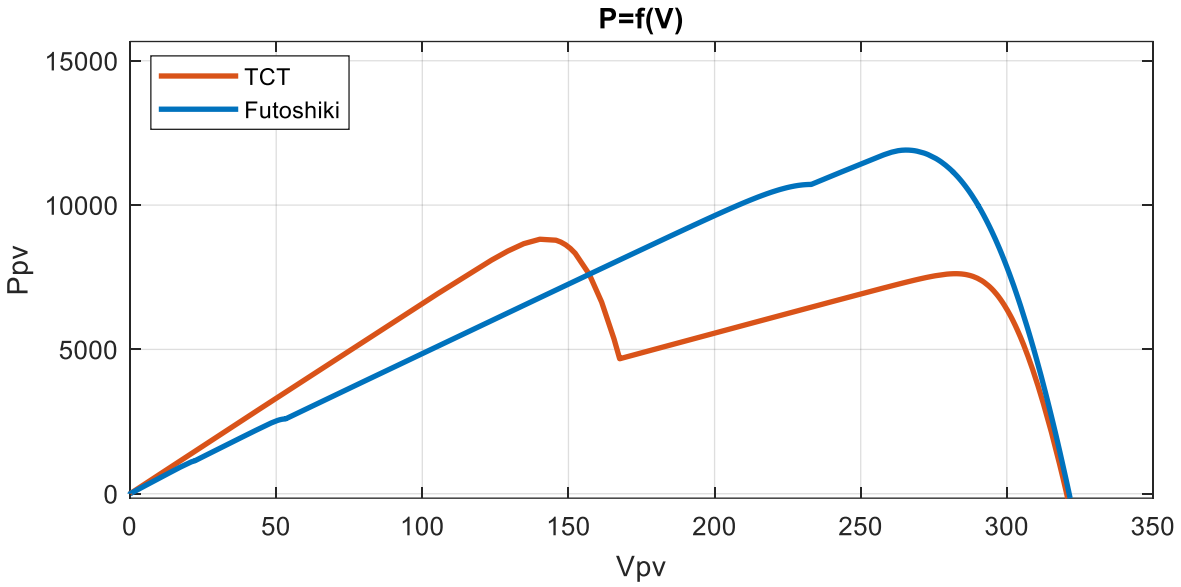

Figure III 8 (9*9) P-V characteristics of different Configuring under partial shading (SW)

A PV array's power, voltage, and current distribution across each row is shown in Table III V. According to Table III V, the power produced at GMPP in the TCT and Futoshiki configurations is 42.30 VmIm and 55.80 VmIm, respectively. Therefore, the recommended design's theoretically projected power gain over TCT is 31.99%. The highest power generated by the TCT and the recommended design are 8817 W and 11910 W, respectively, as shown in Figure III 8. The maximum power output of the proposed arrangement is thus 35.08% higher than that of the TCT setup.

III.6.2 (9*9) Long and wide Shading Condition (LW):

PV array modules get four different types of solar irradiation, as shown in (matrix), including 940 W/m2, 720 W/m2, 550 W/m2, and 200 W/m2. The various irradiation values for this case are illustrated in the following matrix:

$$L_{9\times9} = \begin{bmatrix} 940 & 940 & 940 & 940 & 940 & 720 & 720 & 720 & 720 \\ 940 & 940 & 940 & 940 & 940 & 720 & 720 & 720 & 720 \\ 940 & 940 & 940 & 940 & 940 & 720 & 720 & 720 & 720 \\ 940 & 940 & 940 & 940 & 940 & 720 & 720 & 720 & 720 \\ 940 & 940 & 940 & 940 & 940 & 720 & 720 & 720 & 720 \\ 550 & 550 & 550 & 550 & 550 & 200 & 200 & 200 & 200 \\ 550 & 550 & 550 & 550 & 550 & 200 & 200 & 200 & 200 \\ 550 & 550 & 550 & 550 & 550 & 200 & 200 & 200 & 200 \\ 550 & 550 & 550 & 550 & 550 & 200 & 200 & 200 & 200 \end{bmatrix} {}^{w}/_{m^2}\ a\ T = 25°$$

(TCT 9*9)

$$L_{9\times9} = \begin{bmatrix} 550 & 940 & 550 & 940 & 940 & 720 & 200 & 720 & 200 \\ 940 & 550 & 940 & 550 & 940 & 720 & 200 & 200 & 720 \\ 940 & 550 & 940 & 550 & 550 & 200 & 720 & 720 & 720 \\ 940 & 940 & 940 & 940 & 550 & 720 & 200 & 200 & 200 \\ 940 & 550 & 940 & 550 & 940 & 200 & 720 & 200 & 720 \\ 940 & 940 & 550 & 940 & 550 & 720 & 200 & 200 & 720 \\ 550 & 940 & 550 & 940 & 940 & 200 & 720 & 720 & 200 \\ 550 & 940 & 550 & 550 & 550 & 720 & 720 & 720 & 720 \\ 550 & 550 & 940 & 940 & 940 & 200 & 720 & 720 & 200 \end{bmatrix} {}^{w}/_{m^2}\ a\ T = 25°$$

(Shade dispersion with Futoshiki 9*9)

the following equations may be used to determine the current flowing through each row of a PV array.

For TCT

$$\mathbf{IR1 = IR2 = IR3 = IR4 = IR5} \quad \text{(III.29)}$$

$$\mathbf{IR1 = 5\ \times 0.94Im + 4\ \times 0.72Im = 7.58Im} \quad \text{(III.30)}$$

$$\mathbf{IR6 = IR7 = IR8 = IR9 = 5\ \times 0.55Im + 5\ \times 0.2Im = 3.55Im} \quad \text{(III.31)}$$

For futoshiki:

$$\mathbf{IR1 = IR2 = IR5 = IR6 = IR7 = IR9} \quad \text{(III.32)}$$

$$\mathbf{IR1 = 3 \times 0.94Im + \ 2 \times 0.72Im + 2\ \times 0.2Im + \ 2 \times 0.55Im = 5.76Im} \quad \text{(III.33)}$$

$$\mathbf{IR3 = 2\ \times 0.94Im + \ 2 \times 0.72Im + 0.2Im + \ 3 \times 0.55Im = 5.37Im} \quad \text{(III.34)}$$

$$\mathbf{IR4 = 4\ \times 0.94Im + 3 \times 0.2Im + \ 0.55Im + 0.72Im = 5.43Im} \quad \text{(III.35)}$$

$$\mathbf{IR8 = 0.94Im + 4 \times 0.55Im + 4 \times 0.72Im = 6.02Im} \quad \text{(III.36)}$$

Table III-VI GMPP, LW shading situation, in TCT and futoshiki setup (9*9)

Long and wide Shading Condition (LW)					
TCT configuration			Futoshiki configuration		
*IR	Array Voltage (V)	Array Power (P)	*IR	Array Voltage (V)	Array Power (P)
IR1 7.58 Im	Vm	07.58 VmIm	IR1 5.76 Im	Vm	05.76 VmIm
IR2 7.58 Im	2Vm	15.16 VmIm	IR2 5.76 Im	2Vm	11.52 VmIm
IR3 7.58 Im	3Vm	22.74 VmIm	IR3 5.37 Im	3Vm	16.11 VmIm
IR4 7.58 Im	4Vm	30.32 VmIm	IR4 5.43 Im	4Vm	21.72 VmIm
IR5 7.58 Im	5Vm	37.90 VmIm	IR5 5.76 Im	5Vm	28.80 VmIm
IR6 3.55 Im	6Vm	21.30 VmIm	IR6 5.76 Im	6Vm	34.56 VmIm
IR7 3.55 Im	7Vm	24.70 VmIm	IR7 5.76 Im	7Vm	40.32 VmIm
IR8 3.55 Im	8Vm	28.00 VmIm	IR8 6.02 Im	8Vm	48.16 VmIm
IR9 3.55 Im	9Vm	31.50 VmIm	IR9 5.76 Im	9Vm	51.84 VmIm

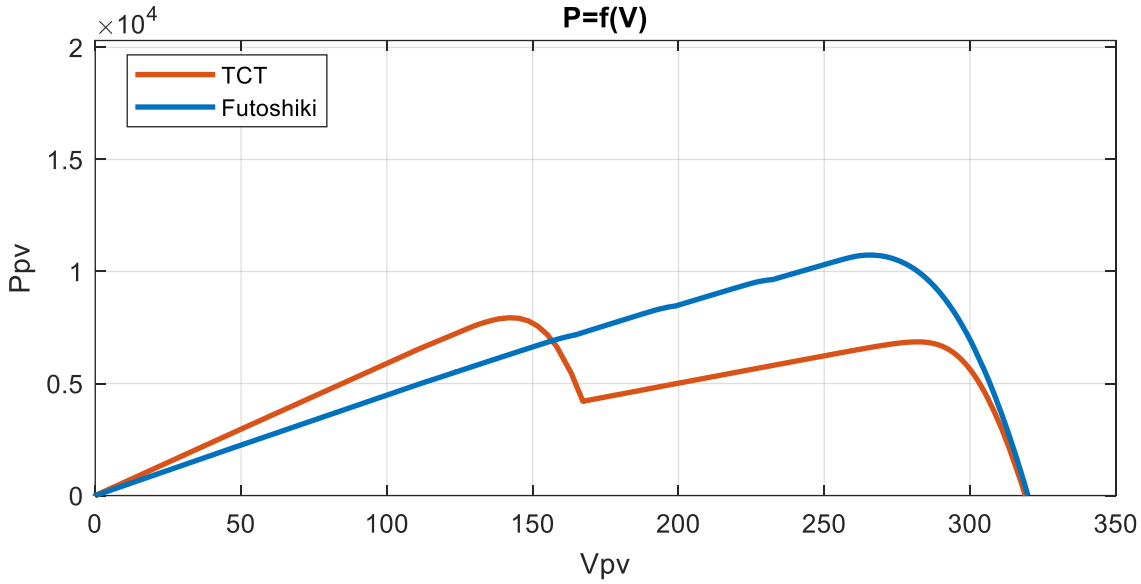

Figure III 9 (9*9) P-V characteristics of different Configuring under partial shading (LW)

A PV array's power, voltage, and current distribution across each row is shown in Table III VI. According to Table III VI the power produced at GMPP in the TCT and Futoshiki configurations is 37.90 VmIm and 51.84 VmIm, respectively. Therefore, the recommended design's theoretically projected power gain over TCT is 36.78%. The highest power generated by the TCT and the recommended design are 7936W and 10730W, respectively, as shown in Figure III 9. The maximum power output of the proposed arrangement is thus 35.08% higher than that of the TCT setup.

III.6.3 (9*9) Short and narrow Shading Condition (SN):

PV array modules are exposed to three different forms of solar irradiation, as depicted in the matrix (matrix), including 940 W/m2, 550 W/m2, and 470 W/m2. The various irradiation values for this case are represented in the matrix below:

$$L_{9\times9} = \begin{bmatrix} 940 & 940 & 940 & 940 & 940 & 940 & 940 & 940 & 940 \\ 940 & 940 & 940 & 940 & 940 & 940 & 940 & 940 & 940 \\ 940 & 940 & 940 & 940 & 940 & 940 & 940 & 940 & 940 \\ 940 & 940 & 940 & 940 & 940 & 940 & 940 & 940 & 940 \\ 940 & 940 & 940 & 940 & 940 & 940 & 940 & 940 & 940 \\ 940 & 940 & 940 & 940 & 940 & 470 & 470 & 470 & 470 \\ 940 & 940 & 940 & 940 & 940 & 470 & 470 & 470 & 470 \\ 940 & 940 & 940 & 940 & 940 & 550 & 550 & 550 & 550 \\ 940 & 940 & 940 & 940 & 940 & 550 & 550 & 550 & 550 \end{bmatrix} {}^{w}/_{m^2}\ a\ T = 25°$$

(TCT 9*9)

$$L_{9\times9} = \begin{bmatrix} 940 & 940 & 940 & 940 & 940 & 940 & 550 & 940 & 470 \\ 940 & 940 & 940 & 940 & 940 & 940 & 550 & 470 & 940 \\ 940 & 940 & 940 & 940 & 940 & 470 & 940 & 940 & 940 \\ 940 & 940 & 940 & 940 & 940 & 940 & 470 & 550 & 550 \\ 940 & 940 & 940 & 940 & 940 & 550 & 940 & 470 & 940 \\ 940 & 940 & 940 & 940 & 940 & 940 & 470 & 550 & 940 \\ 940 & 940 & 940 & 940 & 940 & 550 & 940 & 940 & 470 \\ 940 & 940 & 940 & 940 & 940 & 940 & 940 & 940 & 940 \\ 940 & 940 & 940 & 940 & 940 & 470 & 940 & 940 & 550 \end{bmatrix} {}^{w}/_{m^2}\ a\ T = 25°$$

(Shade dispersion with Futoshiki 9*9)

the following equations may be used to determine the current flowing through each row of a PV array.

For TCT:

$$\mathbf{IR1 = IR2 = IR3 = IR4 = IR5 = 9\ \times 0.94Im = 8.46Im} \quad \text{(III.37)}$$

$$\mathbf{IR6 = IR7 = 5\ \times 0.94Im + 4 \times 0.47Im = 6.58Im} \quad \text{(III.38)}$$

$$\mathbf{IR8 = IR9 = 5\ \times 0.94Im + 4 \times 0.55Im = 6.9Im} \quad \text{(III.39)}$$

For futoshiki:

$$\mathbf{IR1 = IR2 = IR5 = IR6 = IR7 = IR9} \quad \text{(III.40)}$$

$$\mathbf{IR1 = 7\ \times 0.94Im + 0.47Im + 0.55Im = 7.6Im} \quad \text{(III.41)}$$

$$\mathbf{IR3 = 8\ \times 0.94Im + 0.47Im = 7.99Im} \quad \text{(III.42)}$$

$$\mathbf{IR4 = 6\ \times 0.94Im + 0.47Im + 2\ \times 0.55Im = 7.21Im} \quad \text{(III.43)}$$

$$\mathbf{IR8 = 9 \times 0.94Im = 8.46Im} \quad \text{(III.44)}$$

Table III-VII GMPP, SN shading situation, in TCT and futoshiki setup (9*9)

Short and narrow Shading Condition (SN)					
TCT			Futoshiki		
*IR	Array Voltage (V)	Array Power (P)	*IR	Array Voltage (V)	Array Power (P)
IR1 8.46 Im	Vm	08.46 VmIm	IR1 7.60 Im	Vm	07.60 VmIm
IR2 8.46 Im	2Vm	16.20 VmIm	IR2 7.60 Im	2Vm	15.20 VmIm
IR3 8.46 Im	3Vm	25.38 VmIm	IR3 7.99 Im	3Vm	23.97 VmIm
IR4 8.46 Im	4Vm	33.84 VmIm	IR4 7.21 Im	4Vm	28.84 VmIm
IR5 8.46 Im	5Vm	42.30 VmIm	IR5 7.60 Im	5Vm	38.00 VmIm
IR6 6.58 Im	6Vm	39.48 VmIm	IR6 7.60 Im	6Vm	45.60 VmIm
IR7 6.58 Im	7Vm	46.06 VmIm	IR7 7.60 Im	7Vm	53.20 VmIm
IR8 6.90 Im	8Vm	55.20 VmIm	IR8 8.46 Im	8Vm	67.68 VmIm
IR9 6.90 Im	9Vm	62.10 VmIm	IR9 7.60 Im	9Vm	68.40 VmIm

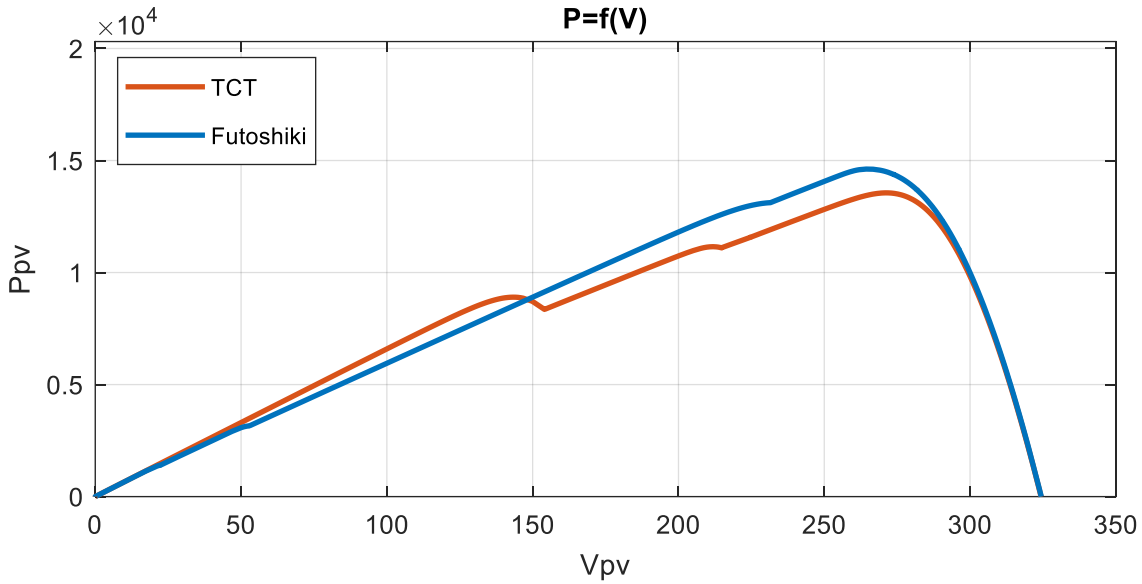

Figure III 10 (9*9) P-V characteristics of different Configuring under partial shading (SN)

A PV array's power, voltage, and current distribution across each row is shown in Table III VII. According to Table III VII the power produced at GMPP in the TCT and Futoshiki configurations is 62.10 VmIm and 68.40 VmIm, respectively. Therefore, the recommended design's theoretically projected power gain over TCT is 10.14%. The highest power generated by the TCT and the recommended design are 13560W and 14620W, respectively, as shown in Figure III 10. The maximum power output of the proposed arrangement is thus 7.81% higher than that of the TCT setup.

III.7 CONCLUSION:

The configuration performance of TCT photovoltaic panels in shading conditions is studied and analyzed using a single diode model in MATLAB / Simulink. In this work, four shadow patterns are dealt with. The results collected demonstrate how well the futoshiki configuration, which is taught based on shadow dispersion to enhance total PV performance under various shading situations, performs. The results of thorough research and examination of the configurations show that the type and placement of the shading pattern have a significant impact on the decision of the best and most appropriate design. Overall, it is believed that the suggested futoshiki arrangement significantly outperforms conventional PV layouts in terms of photovoltaic panel performance. Aside from that, the results prove that this approach can ensure a considerable improvement in the electrical performance of PV panels.

General conclusion

General conclusion:

The purpose of this project is to study, model and simulate different configurations of photovoltaic panels under partial shade. In the beginning, concepts about photovoltaic energy, solar irradiation, photoelectric effect, photovoltaic cell and principle of operation are presented. And we modeled the photovoltaic cell, the different factors affecting the I-V and P-V properties. In the second chapter, we introduced the different configurations that exist, and used the single diode model to study and model the effect of partial shading on Parallel Series (SP), Linked Bridge (BL), Honeycomb (HC) and Total-Cross-Tied (TCT) configurations according to for the simulation results obtained, we can say: The Cross-Tied (TCT) configuration offers the best performance. In the third chapter, we propose the Futoshiki technique to disperse shading and increase power generation in partially shaded PV arrays. It involves rearranging the physical location of modules without changing electrical connections. The proposed configuration consistently achieves maximum power compared to the traditional TCT configuration under different shading patterns and array sizes. It is a cost-effective and simpler installation process without the need for switches and sensors.

The suggested arrangement is less expensive and easier to install because it doesn't call for switches or sensors. Therefore, taking into account all of the aforementioned information, the suggested approach will assist the PV installer in obtaining more power from the PV source while it is partially shaded.

Future work aims to:

1. Enhanced Solar Data Modeling: Improve the accuracy and granularity of solar data modeling to account for local weather conditions, shading from nearby objects, and dynamic changes in solar irradiation intensity throughout the day. This can help refine the optimization process and ensure more precise placement of PV panels.
2. Integration of Machine Learning Techniques: Explore the integration of machine learning techniques, such as reinforcement learning or genetic algorithms, to optimize the Futoshiki algorithm for PV panel reconfiguration. By allowing the algorithm to learn from past solutions and adapt to different scenarios, it can achieve more efficient and effective panel arrangements.
3. Multi-objective Optimization: Extend the optimization framework to consider multiple objectives simultaneously, such as maximizing energy production, minimizing installation costs, and reducing the environmental impact. This can involve developing

sophisticated optimization algorithms that can handle multiple conflicting objectives and provide a range of optimal solutions for decision-making.

4. Dynamic Reconfiguration: Investigate the feasibility of dynamically reconfiguring PV panel layouts based on real-time data. By integrating sensors and monitoring systems, the algorithm can continuously adjust the panel configuration to adapt to changing environmental conditions, such as cloud cover or the growth of surrounding vegetation.

5. Incorporate Panel-Level Characteristics: Take into account the individual characteristics of PV panels, such as their efficiency, temperature coefficients, and degradation rates. By incorporating these factors into the reconfiguration algorithm, it can optimize the placement and configuration of panels to minimize performance degradation and maximize their operational lifespan.

6. Scalability and Large-Scale Applications: Address the challenges associated with scaling up the optimization framework for large-scale PV installations, such as utility-scale solar farms or urban solar projects. Develop algorithms and techniques that can handle the complexity of massive panel arrays and provide efficient and scalable solutions.

7. Cost Analysis and Economic Considerations: Conduct in-depth economic analysis to evaluate the financial viability and cost-effectiveness of different PV panel reconfiguration strategies. Consider factors such as upfront installation costs, maintenance expenses, and the overall return on investment to guide decision-making in real-world applications.

8. Collaborative Optimization: Explore collaborative optimization approaches that involve multiple stakeholders, such as system operators, energy providers, and policymakers. Incorporate their preferences, constraints, and objectives into the reconfiguration algorithm to ensure the developed solutions align with broader energy planning goals.

9. Environmental Impact Assessment: Conduct comprehensive life cycle assessments to evaluate the environmental impact of different PV panel reconfiguration strategies. Consider factors such as embodied energy, carbon emissions, and potential ecological effects to ensure that the optimization process promotes sustainable and environmentally friendly solutions.

10. Real-World Validation and Case Studies: Validate the effectiveness of the optimized PV panel reconfiguration strategies through real-world case studies and field

trials. Collaborate with industry partners and deploy the optimized configurations in operational solar installations to assess their performance, validate the algorithm's accuracy, and gather feedback for further improvements.

By exploring these research directions, scientists and researchers can contribute to advancing the optimization of the Futoshiki algorithm for PV panel reconfiguration, ultimately leading to more efficient and effective solar energy systems.

Bibliographic

1. Handley, S.M.L. *'It is entirely doable, and it is doable fast': Experts on how to navigate the energy transition*. 2021 [cited 04/29/2023; Available from: https://www.cnbc.com/2021/11/22/climate-how-to-navigate-the-energy-transition-away-from-fossil-fuels.html.
2. Escap, U., *Low carbon green growth roadmap for Asia and the Pacific: Turning resource constraints and the climate crisis into economic growth opportunities.* 2012.
3. Norberto, C., C.N. Gonzalez-Brambila, and Y. Matsumoto, *Systematic analysis of factors affecting solar PV deployment.* Journal of Energy Storage, 2016. **6**: p. 163-172.
4. Becquerel's, E., *electrochemical actinometer.* Archives des sciences, 2005. **58**: p. 147-156.
5. Kreider, J.F. and F. Kreith, *Solar energy handbook.* 1981.
6. Ranabhat, K., et al., *An introduction to solar cell technology.* Journal of Applied Engineering Science, 2016. **14**(4): p. 481-491.
7. Schiller, E. and B.S. Sy, *Le pompage photovoltaïque, manuel de cours à l'intention des ingénieurs et des techniciens.* Université d'Ottawa, 1998. **1**.
8. KHEDDIOUI, A., E.M. EL OUIQARY, and M. SMIEJ, *Estimation of the global horizontal solar irradiation GHI for the Moroccan national territory from meteorological satellite images of the Second Generation Meteosat series MSG.* European Journal of Molecular & Clinical Medicine, 2021. **8**(3): p. 2814-2826.
9. Marashli, A., et al., *Impact of Accumulated Dust on Performance of Two Types of Photovoltaic Cells: Evidence from the South of Jordan.* International Journal of Renewable Energy Development, 2022. **11**(2).
10. Dusanter, C. *Energie solaire : définition et différents types d'exploitation*. 2023 01 May 2023]; Available from: https://opera-energie.com/energie-solaire/.
11. Littlefair, P., *Passive solar urban design: ensuring the penetration of solar energy into the city.* Renewable and Sustainable Energy Reviews, 1998. **2**(3): p. 303-326.
12. Rathore, N., et al., *A comprehensive review of different types of solar photovoltaic cells and their applications.* International Journal of Ambient Energy, 2021. **42**(10): p. 1200-1217.
13. Zheng, M., et al., *Photovoltaic effect and tribovoltaic effect at liquid-semiconductor interface.* Nano Energy, 2021. **83**: p. 105810.
14. Fraas, L.M., *History of solar cell development.* Low-cost solar electric power, 2014: p. 1-12.
15. Sharma, S. and R. Rishi, *A comparative analysis on different types of Photovoltaic Cells.* International Journal of Next-Generation Computing, 2022. **13**(3).
16. Xu, Z., et al., *A new uniformity coefficient parameter for the quantitative characterization of a textured wafer surface and its relationship with the photovoltaic conversion efficiency of monocrystalline silicon cells.* Solar Energy, 2019. **191**: p. 210-218.
17. Mesquita, D.d.B., et al. *A review and analysis of technologies applied in PV modules*. in *2019 IEEE PES Innovative Smart Grid Technologies Conference-Latin America (ISGT Latin America)*. 2019. IEEE.
18. Chen, D., et al., *Evidence of an identical firing-activated carrier-induced defect in monocrystalline and multicrystalline silicon.* Solar Energy Materials and Solar Cells, 2017. **172**: p. 293-300.

19. Aberle, A.G., *Thin-film solar cells.* Thin solid films, 2009. **517**(17): p. 4706-4710.
20. ecotechnica. *Which solar panels are better: monocrystalline, polycrystalline or thin film*. 2021 20/03/2023]; Available from: https://ecotechnica.com.ua/stati/5151-kakie-solnechnye-paneli-luchshe-monokristallicheskie-polikristallicheskie-ili-tonkoplenochnye.html#amorph.
21. Hatem, D., F. Nemmar, and M. Belkaid, *Cellules solaires organiques: choix des matériaux, structures des dispositifs et amélioration du rendement et de la stabilité.* Journal of Renewable Energies, 2009. **12**(1): p. 77–86-77–86.
22. Pedro, M.C. *Modelling of shading effects in photovoltaic optimization*. 2016.
23. Masters, G.M., *Renewable and efficient electric power systems*. 2013: John Wiley & Sons.
24. Chahid, E., et al., *Extraction des paramètres électriques d'une cellule solaire organique à base de (P3HT: PCBM).* REVUE DE L'ENTREPRENEURIAT ET DE L'INNOVATION, 2018. **2**(6).
25. Fouad, M., L.A. Shihata, and E.I. Morgan, *An integrated review of factors influencing the perfomance of photovoltaic panels.* Renewable and Sustainable Energy Reviews, 2017. **80**: p. 1499-1511.
26. Dittrich, T., *Basic Characteristics andCharacterization of Solar Cells.* Materials Concepts for Solar Cells, 2018. **3**.
27. SHIHAB, S. and M. RASHEED, *Modelling and Simulation of Solar Cell Mathematical Model Parameters Determination Based on Different Methods.* Insight-Mathematics, 2019. **1**(1).
28. Djerdir, A., K. Elkadri, and A. Miraoui, *Alimentation par biberonnage solaire photovoltaïque d'une chaîne de motorisation électrique.* Revue des énergies renouvelables, 2006. **9**(2): p. 63-74.
29. Abbassen, L., *Etude de la connexion au réseau électrique d'une centrale photovoltaique*. 2011, Université Mouloud Mammeri.
30. Hasan, K., et al., *Effects of different environmental and operational factors on the PV performance: A comprehensive review.* Energy Science & Engineering, 2022. **10**(2): p. 656-675.
31. Klugmann-Radziemska, E., *The environmental benefits of photovoltaic systems: The impact on the environment in the production of photovoltaic systems: With a focus on metal recovery.* 2022.
32. Abid, M.K., et al., *Environmental Impacts of the Solar Photovoltaic Systems in the Context of Globalization.* Ecol. Eng. Environ. Technol, 2023. **24**: p. 231-240.
33. Lopez, R.P. and J. Ferreira, *Identifying spatio-temporal hotspots of human activity that are popular non-work destinations.* Environment and Planning B: Urban Analytics and City Science, 2021. **48**(3): p. 433-448.
34. Raghuraman, B.D.R.A.a.K.S.a.B. *Hot spots: Causes and effects*. 2017 01/04/2023]; Available from: https://pv-magazine-usa.com/2017/08/22/hot-spots-causes-and-effects/.
35. Dhakshinamoorthy, M., et al., *Bypass diode and photovoltaic module failure analysis of 1.5 kW solar PV array.* Energy Sources, Part A: Recovery, Utilization, and Environmental Effects, 2022. **44**(2): p. 4000-4015.
36. Nunes, H., et al., *Bypass diode effect and photovoltaic parameter estimation under partial shading using a hill climbing neural network algorithm.* Frontiers in Energy Research, 2022. **10**(837540): p. 10.3389.
37. Sycomoreen. *LE PHOTOVOLTAÏQUE EN FRANCE*. 2010 15/04/2023]; Available from: https://www.econologie.com/file/habitat/Solaire_PV_synthese.pdf.

38. Al Mansur, A., M.R. Amin, and K.K. Islam. *Determination of module rearrangement techniques for non-uniformly aged PV arrays with SP, TCT, BL and HC configurations for maximum power output*. in *2019 International Conference on Electrical, Computer and Communication Engineering (ECCE)*. 2019. IEEE.

39. Picault, D., *Reduction of mismatch losses in grid-connected photovoltaic systems using alternative topologies*. 2010, Institut National Polytechnique de Grenoble-INPG.

40. Villa, L.F.L., et al., *Maximizing the power output of partially shaded photovoltaic plants through optimization of the interconnections among its modules.* IEEE Journal of Photovoltaics, 2012. **2**(2): p. 154-163.

41. Yadav, A.S. and V. Mukherjee, *Line losses reduction techniques in puzzled PV array configuration under different shading conditions.* Solar Energy, 2018. **171**: p. 774-783.

42. Haraguchi, K., *The number of inequality signs in the design of Futoshiki puzzle.* Journal of information processing, 2013. **21**(1): p. 26-32.

43. SUNGUR, B.B., *An Integer Programming Formulation For The Futoshiki Puzzle.* International Review of Economics and Management, 2022. **10**(2): p. 38-49.

44. Sahu, H.S., S.K. Nayak, and S. Mishra, *Maximizing the power generation of a partially shaded PV array.* IEEE journal of emerging and selected topics in power electronics, 2015. **4**(2): p. 626-637.

45. *Futoshiki*. 2023 [cited 05/20/2023; Available from: https://www.futoshiki.com/.

APPENDICES

characteristics	Value
Maximum Power (W)	213.15
Open circuit voltage Voc (V)	36.3
Voltage at maximum power point Vmp (V)	29
Short-circuit current Isc (A)	7.84
Current at maximum power point Imp (A)	7.35
Cells per module (N cell)	60

ملخص:

تعتبر الطاقة المولدة من المولدات الكهروضوئية إلى حد ما قليل مقارنتا بغيرها، وكفاءتها منخفضة بسبب تذبذب كمية الطاقة المنتجة المرتبطة بالظروف الجوية (درجة الحرارة، مستوى الإشعاع ...)، وبالتالي يجب تحسينها.

في هذا العمل، نجري دراسة في تكوينات المقترحة(SP BL HC TCT) من اجل التحسين قوة المولد الكهروضوئي غير مضاء بشكل موحد، العمل الذي قمنا به بعد ذلك هو التحسين من تكوينات TCT من خلال تقنية futoshiki المستخدمة من اجل تشتيت تأثير التظليل.

من خلال محاكاة سيناريوهات التظليل الجزئي لمولد كهروضوئي ومقارنة النتائج قبل إعادة التكوين وبعدها، تم تأكيد فعالية هذه الاستراتيجية.

Résumé :

L'énergie générée par les générateurs photovoltaïques est quelque peu faible par rapport aux autres, et son efficacité est faible en raison de la fluctuation de la quantité d'énergie produite liée aux conditions météorologiques (température, niveau de rayonnement...), et doit donc être améliorée.

Dans ce travail, nous menons une étude dans les configurations proposées (SP BL HC TCT) dans le but d'améliorer la puissance du générateur photoélectrique qui n'est pas uniformément éclairé, le travail que nous avons fait après c'est l'optimisation des configurations TCT par futoshiki technique utilisée pour disperser l'effet d'ombrage.

En simulant des scénarios d'ombrage partiel pour un générateur photovoltaïque et en comparant les résultats avant et après reconfiguration, l'efficacité de cette stratégie a été confirmée.

Abstract:

The energy generated from photovoltaic generators is somewhat low compared to others, and its efficiency is low due to the fluctuation of the amount of energy produced related to weather conditions (temperature, irradiation level...), and therefore it must be improved.

In this work, we conduct a study in the proposed configurations (SP BL HC TCT) in order to improve the power of the photoelectric generator is not uniformly illuminated, the work that we have done after that is the optimization of the TCT configurations by futoshiki technique used in order to disperse the shading effect.

By simulating partial shading scenarios for a photovoltaic generator and comparing the results before and after reconfiguration, the effectiveness of this strategy was confirmed.